Design and Fabrication of a Positioning System for an Intravascular Electrode System

by

Mark Nolette

B.Sc. (Mech. Engineering), Université de Sherbrooke, 2009

THESIS SUBMITTED IN PARTIAL FULFILLMENT
OF THE REQUIREMENTS FOR THE DEGREE OF
MASTER OF SCIENCE

in the
Department of Biomedical Physiology and Kinesiology
Faculty of Science

SIMON FRASER UNIVERSITY

Spring 2012

Approval

Name: **Mark Nolette**

Degree: **Master of Science**

Title of Thesis: ***Design and fabrication of a positioning system for an intravascular electrode system***

Examining Committee:

Chair: Angela Brooks-Wilson Associate Professor

Joaquin Andres Hoffer
Professor
Senior Supervisor

Carlo Menon
Assistant Professor
Supervisor

Steve Robinovitch
Professor
External Examiner

Date Defended/Approved: March 6th 2012

Partial Copyright Licence

Ethics Statement

The author, whose name appears on the title page of this work, has obtained, for the research described in this work, either:

a. human research ethics approval from the Simon Fraser University Office of Research Ethics,

or

b. advance approval of the animal care protocol from the University Animal Care Committee of Simon Fraser University;

or has conducted the research

c. as a co-investigator, collaborator or research assistant in a research project approved in advance,

or

d. as a member of a course approved in advance for minimal risk human research, by the Office of Research Ethics.

A copy of the approval letter has been filed at the Theses Office of the University Library at the time of submission of this thesis or project.

The original application for approval and letter of approval are filed with the relevant offices. Inquiries may be directed to those authorities.

Simon Fraser University Library
Burnaby, British Columbia, Canada

update Spring 2010

Abstract

Precise placement of intravascular leads is a vital requirement for transvascular neurostimulation as it determines the nerve selectivity and efficiency of stimulation. With the previous positioning method relying on ruler measurements, an electronic position sensor system was designed to minimize placement time, increase accuracy, reproducibility and allow for integration into a control unit system.

To keep track of each electrode array, the developed sensor uses one linear membrane potentiometer for each lead. A plastic bead is fitted on each lead and as the bead is lightly squeezed into the membrane potentiometer, the potentiometer resistance changes proportionally to a bead position. The electrode position can therefore be inferred from this measurement. This system is simple, inexpensive and provides an absolute position measurement. This concept is also expected to be easily made into commercial product because of its compact and intuitive nature.

Keywords: Intravascular Catheter; Displacement Sensor; Neurostimulation

“It ain't about the dollar or trying to go fast

Unless you take pride in what you're doing, it won't last

Craftsmanship is a quality that some lack

You got to give people a reason for them to come back”

- *Richard Terfry*

Acknowledgements

Even if there is only one name on the spine of this thesis, a lot of people have helped make it what it is. From close or far, all these people have contributed either to its content or supported my sanity throughout the project.

For providing me with the chance to work on this project, I owe Dr. Andy Hoffer a great deal of appreciation. By welcoming me from so far, and giving me the responsibility of this important project, Dr. Hoffer has put great faith in me, and I hope not to have fallen short of his expectations.

During my time in the Simon Fraser University, many people provided support both in and outside of the lab. First, for welcoming me to the province, the lab and the project, I am very grateful I had Jessica Tang here to help. Also, I have to thank Jessica for being my sounding board for every crazy idea I've had for the two years I worked on this project. Marcelo and Bernard also deserve my gratitude for their assistance in making sense of everything electronics-related. Thanks to Marcelo, I learned that drills are not only made for drilling.

Even though he arrived late on the project, the presence of Viral Thakkar has benefitted me extensively. By giving me tips based on his experience, I have learned things that I would not have had access to otherwise. Our discussions also led to various ideas of bold design changes. Some of which made their way into this document.

Sometimes support also comes from unexpected places. For example, receiving a Ziploc bag with homemade cookies in them can lead to a major improvement in a prototype. Thanks to Lauren Tindale for that indirect contribution and all of the proofreading.

Lastly, I have to thank Susie Nugent, our graduate studies coordinator, who helped and guided me from the first time I saw her, up until the last words of this document were written. Susie, you're awesome.

Table of Contents

List of Tables

List of Figures

List of Acronyms

ECG	Electrocardiography
EMG	Electromyography
ICU	Intensive Care Unit
IV	Intravascular
IVC	Intravascular Catheter
MV	Mechanical Ventilation
RoHS	Restriction of Hazardous Substances Directive

1. Introduction

Mechanical ventilation saves lives every day, but its use over multiple days can be the source of great harm and sometimes even death. By unloading the respiratory muscles entirely, mechanical ventilation induces atrophy in the main muscle of respiration, the diaphragm. This atrophy can therefore delay the patient's full recovery by keeping prolonging ventilator dependence. To solve this problem, the Neurokinesiology lab is developing an alternative technique involving transvascular neurostimulation.

The two phrenic nerves, responsible for diaphragmatic contraction, cross the upper chest vasculature at specific sites. With an electrode positioned near each of these sites, it is possible to electrically stimulate the nerves through the walls of the blood vessels. In turn, nerve stimulation induces contractions of the diaphragm, which draws air into the lungs. Additionally, electrical stimulation over an extended period of time provides a training effect on the diaphragm by building or maintaining its strength.

Currently, positioning electrodes in close proximity to where the phrenic nerves cross the vasculature involves a time-consuming mapping process. By sequentially stimulating at different positions in the vein and correlating stimulation efficiency with proximity to a nerve, one can determine the depth at which the lowest charge is necessary for stimulation, which can then be assumed to be in closest proximity to the nerve. However, to accurately map the vessel at different positions, it is necessary to keep track of the lead movement. The method originally used to measure electrode position was a ruler.

To accelerate the positioning process and to move towards the goal of full automation, this project aims to create a position sensor for keeping track of the intravascular lead. In partnership with Lungpacer Medical Inc., this project also aims to create a system easily adaptable for integration into a larger control system.

1.1 Background

In order to understand the need to position a respiratory pacer, it is important to first understand the act of breathing itself and the elements that contribute most to this action.

At a high level, respiration simply involves a change in volume of the thoracic cavity, creating a pressure differential in the lungs, thus pulling air into the lungs. This volume variation and pressure difference is elicited by contraction of the diaphragm and the intercostal muscles. The shortening of the muscles induces a pressure gradient that expands the lungs thus drawing air in and produces inspiration. Subsequently, the muscles relax and the elasticity of the lungs and chest wall brings the thoracic volume back down, passively expelling the inspired air.

1.1.1. Anatomy

The diaphragm muscle, innervated exclusively by the phrenic nerves, is the primary force behind ventilation and is able to maintain a high enough tidal volume to sustain normal ventilation [DiMarco et al, 2004]. The innervation of this muscle is distributed into two halves: The left and right hemidiaphragm, which are respectively innervated by the left and right phrenic nerves. The phrenic nerves originate from the 3rd to 5th cervical nerves and go down to innervate the diaphragm. On its course to the muscle, the right phrenic nerve runs parallel to the lateral side of the superior vena cava, while the left phrenic nerve crosses the subclavian vein on its posterior side before it branches to become the brachiocephalic vein (see Figure 1). Electrical stimulation of these nerves can be analogous to a real breathing command from the brain as it replaces the phrenic nerve's natural drive and thus induces contraction of the diaphragm muscle.

Figure 1: Anatomical view and location of the phrenic nerves

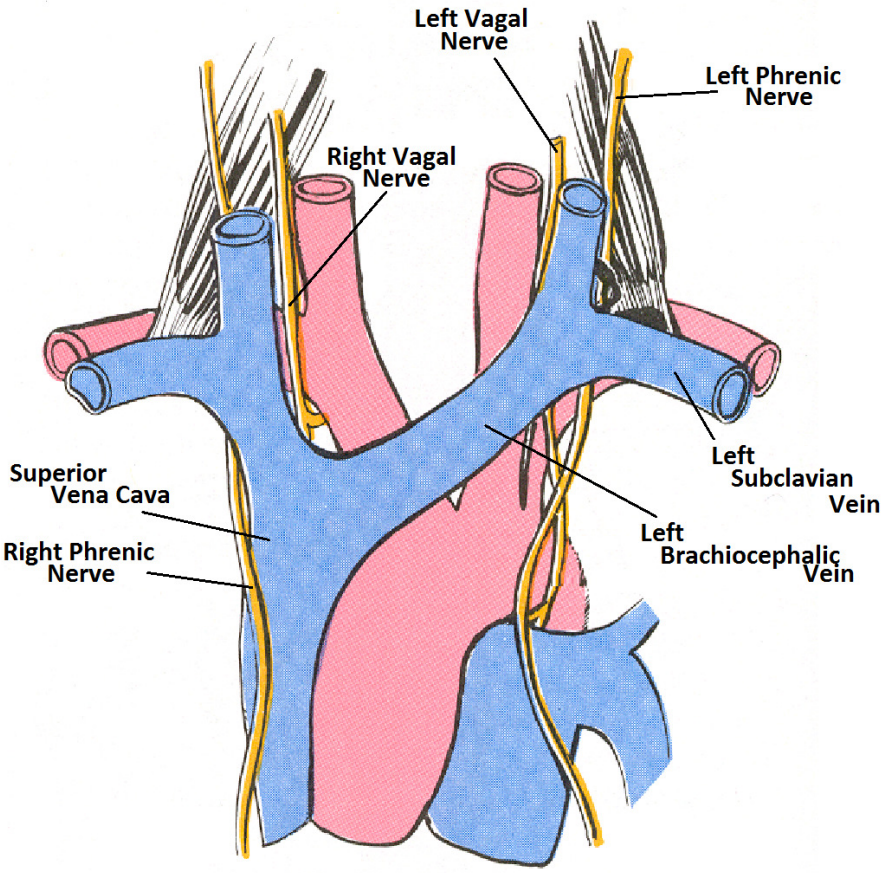

Note: Picture from dartmouth.edu

In proximity to the phrenic nerves, are the vagal nerves. The left vagus nerve crosses the left brachiocephalic vein at a position medial of the left phrenic nerve while the right vagus nerve runs posterior of the superior vena cava. Although the vagus nerve is mainly sensory, it is also responsible for the movement of various abdominal muscles and glands. Namely, it plays a role in the regulation of heart rate, gastrointestinal peristalsis, sweating and muscles involved in speech and swallowing. The most notable effect of vagal neurostimulation that could be a concern is a decrease in heart rate [Groves et al, 2005].

In situations of trauma (amongst others), the brain can stop sending the signals that control diaphragmatic contractions. A common solution to maintain oxygen intake and carbon dioxide expiration is mechanical ventilation (MV). Typically using a tube inserted in the patient's trachea, ventilators can completely replace the function of the respiratory muscles by pushing air into the patient's lungs.

1.1.2. Mechanical Ventilation

Over the years, mechanical ventilators have become an essential [Esteban et al, 2000] part of intensive care units (ICU) around the world, mainly because of their short-term advantages such as ease of installation and lifesaving potential. A few short-term inconveniences also characterize the use of MV, including typically a need for sedation, a risk of infection, and the inability to talk and eat normally. Extended use, however, has shown that serious consequences and significant harm can befall patients who fail to wean from mechanical ventilation [Esteban et al., 2002].

During this period of weakness, it is not uncommon for patients to contract nosocomial infections unrelated to their initial condition, and consequently prolong their stay in the hospital [Dasta et al., 2005]. It is important to understand that this extension of hospital stay can cause serious long-term hazards for the elderly and other vulnerable patient populations. Fast weaning from MV and sedation is therefore crucial to the well-being of patients. However, very few tools are available to accelerate the recovery of diaphragmatic strength other than having the patients achieve periodic short bouts of spontaneous breathing in a hope to retrain the respiratory muscles by exercising them. The patient is, however, put back on MV and sedation as soon as the muscles fatigue. This paradoxical need for the ventilator takes a considerable toll on patients and the health care sector as a whole, thus creating a need for a replacement solution.

Discontinuing ventilatory support is essential to the quick recovery of a patient. However, therapists struggle to determine when a patient is ready to be extubated. The first step that therapists usually follow is to determine if the patient has recovered from acute respiratory failure. From there, the patients can be progressively removed from MV; however, approaches to weaning diverge significantly through the varying degree of aggressiveness used by therapists [MacIntyre, 2001]. Studies on the effectiveness of the different weaning methods often fail to consider the subjectivity of subject recruitment or differences in the variables used to qualify weaning.

Although different methods of weaning produce varying results, all can agree that the duration of ventilator support should be kept to a minimum. As patients passively rely on MV to breathe, their diaphragm muscle starts to atrophy due to inactivation. It has been shown that this disuse atrophy can cause the muscle fibers to decrease in cross-sectional area by 52 to 58% in as little as 18 to 69 hours on mechanical ventilation [Levine et al, 2008]. After such a loss of muscle mass, force generation becomes severely impaired and patients become unable

to breathe independently. In fact, once removed from MV, patients often suffer from a gradual decrease in their ability to breathe because of greater muscle fatigue and decreased endurance associated with the reduced respiratory muscle mass [Lemaire, 1993].

Recently, new mechanical ventilation modes have been created to alleviate this problem [Sassoon et al, 2004]. The most common is known as assist-mode ventilation. By detecting any attempts made by a patient to breathe, this mode attempts to preserve diaphragmatic strength by assisting ventilation rather than replacing it altogether. Although this technology is believed to attenuate ventilator-induced diaphragmatic dysfunction, its efficacy has not yet been shown in humans [Sieck and Mantilla, 2008].

1.1.3. Implantable Ventilation Solutions

Another method currently being used to provide artificial ventilation to patients with permanent ventilatory deficit is phrenic nerve neurostimulation. Under general anaesthesia, electrodes are implanted either directly on the patient's phrenic nerves (Avery Biomedical[1]) or near the junction between the phrenic nerves and diaphragm (Synapse Biomedical[2]). The electrodes are then used to stimulate the nerves using an external control unit.

The Avery Biomedical system has been in use since the early 1970's. It uses a control unit worn by the patient which communicates through the skin. The communication and power transmission is insured by antennas worn on the skin over an implanted receiver. The receiver supplies the stimulation through a highly flexible stainless steel wire, insulated by silicone rubber, with a platinum nerve contact. Positioning of theses electrodes requires surgery under general anaesthesia, which can be performed both cervically and thoracically. The surgery therefore takes a few hours. Using the thoracic approach, the electrodes are implanted on the phrenic nerves as they run alongside the heart. However, the cervical approach is usually preferred because of the superficiality of the nerves in the neck.

[1] From Avery Biomedical official website: http://www.averybiomedical.com/breathing-pacemakers/introduction.html, July 18th, 2011.

[2] From Synapse Biomedical Inc official website: http://www.synapsebiomedical.com/products/neurx.shtml, July 18th 2011

Figure 2: Implanted electrodes and control unit of the Avery Biomedical pacing system

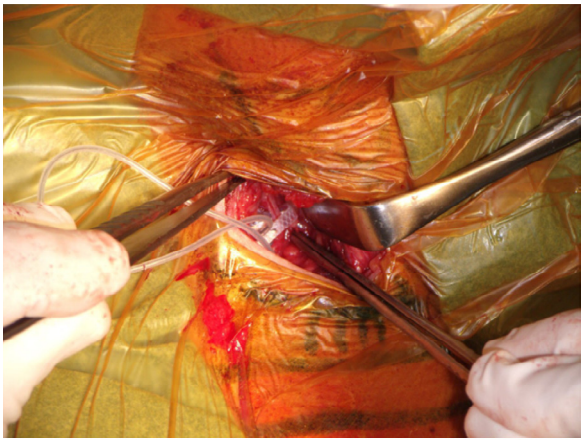

(a)

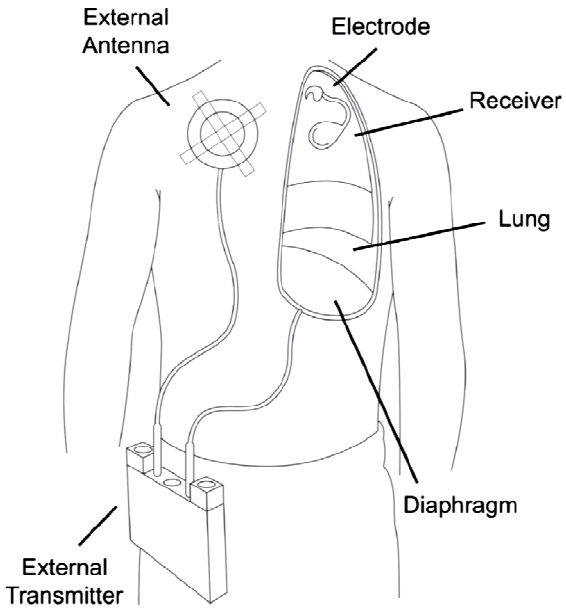

(b)

Note: Pictures from Khong et al, 2010.

A competitor to the Avery system is developed by Synapse Biomedical with the main difference being that stimulation is delivered directly to diaphragm. Multiple long-term electrodes are implanted into the diaphragm at the motor points, in close proximity to the neuromuscular junctions of the phrenic nerves to the diaphragm [Onders et al, 2007]. A laparoscopic procedure is used to implant the system, thus reducing the invasiveness of the surgery. To provide stimulation, the electrodes are all joined into a single cable that crosses the skin and links to an external control unit. The system can then deliver rhythmic stimulation to patients suffering from any of a variety of breathing disorders. An advantage to this system over the Avery system lies in its independence from nerve conductivity. Consequently, this system can then be used in the treatment of patient suffering neurodegenerative disorders such as amyotrophic lateral sclerosis.

Although this therapy can be life-saving, the scope of such a surgery and the associated risks means that this solution is only appropriate for cases of permanent incapacity to provoke spontaneous breathing in a patient healthy enough to endure major surgery under general anaesthesia. The length, cost and invasiveness of these procedures therefore make them unsuitable options to help fragile ICU patients wean from MV.

1.1.4. Transvascular Phrenic Nerve Stimulation

For many years, phrenic nerve stimulation has been known to be possible using a transvascular approach [Ishii et al., 1990]. However, no commercial product using this concept have been developed until Respicardia filed a patent for a system aiming to treat sleep apnea using transvascular phrenic nerve stimulation in 2007.The system proposed by the Minnesota company includes a stimulation electrode, typically placed within one of the cardiophrenic veins. Information about the method of placement and electrode configuration is currently unavailable for confidentiality reasons, but one can assume that the electrodes are at the tip of small leads placed a set fraction of the way down the vein. This assumption is derived from the fact that the phrenic nerve and cardiophrenic vein run parallel to each other (Figure 3). Although less invasive than the phrenic nerve stimulation systems previously mentioned, this system still requires the implantation of a control unit [US2007/0118183].

Figure 3: Cardiophrenic vein location

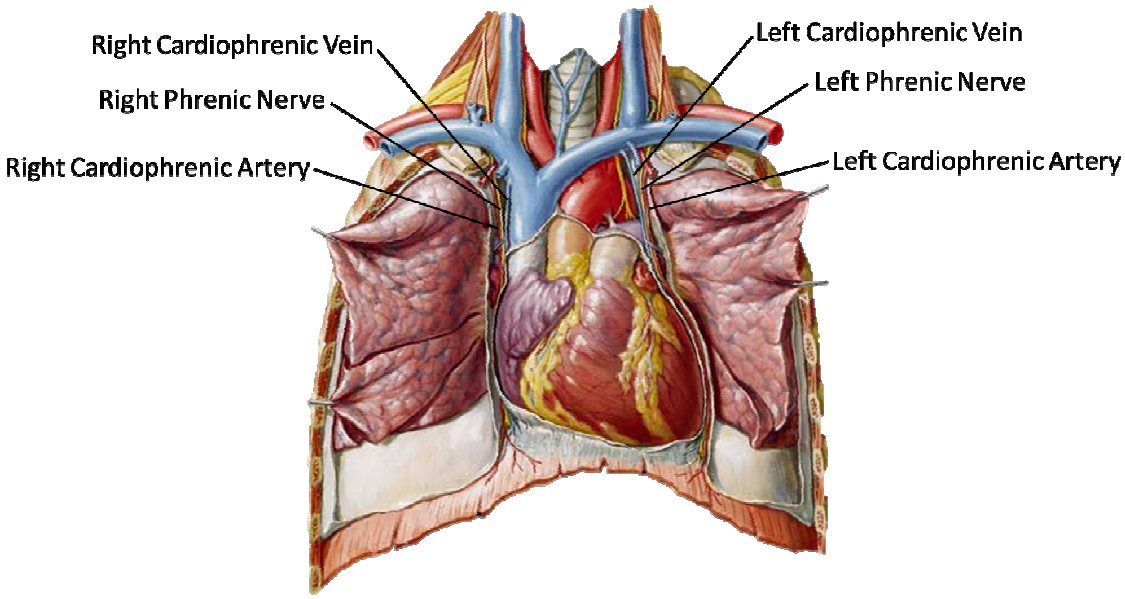

A less-invasive alternative to surgical phrenic nerve stimulation methods is being developed by the Neurokinesiology Lab at Simon Fraser University [Hoffer, 2008; Hoffer et al., 2010]. The proposed solution uses intravenous (IV) electrodes inserted using the Seldinger technique into the left subclavian vein. Each electrode array is then positioned in proximity to a phrenic nerve; the left electrode array is placed in the subclavian vein and while the right electrode is positioned in the superior vena cava. The nerves are then paced through the vessel

wall using an external control unit. By using an intravenous catheter to deliver stimulation, eligibility of patients is greatly improved compared to products where implantation requires full anaesthesia. As well, the majority of patients in the ICU are already fitted with central venous catheters for administration of drugs and retrieval of blood samples.

The therapy delivered by this catheter system is designed to rhythmically stimulate the phrenic nerves in synchrony with the mechanical ventilator. This type of stimulation has been shown to attenuate the positive pressure induced by the ventilator therefore reducing the risk of ventilator induced lung injury [Dreyfuss et al, 1998]. By stimulating in this manner over the course of multiple days, it is believed that the disuse atrophy normally caused by mechanical ventilation may be reduced, prevented or even reversed. Implanted systems such as the Synapse Biomedical or Avery Biomedical System have already helped show that phrenic nerve stimulation can restore muscle strength in atrophied muscles [Glenn et al, 1985, Onders et al., 2007].

An important aspect is the effectiveness of transvascular neurostimulation since it is dependent on the electrode's proximity to the nerve. In terms of IV position, two variables can be controlled to change proximity; the depth of the electrode and the angle at which it is oriented. Through a series of acute experiments using a pig model, the Neurokinesiology lab team was able to map the efficiency of stimulation as a function of electrode depth as shown for example in Figure 4. To qualify efficiency, the notion of threshold stimulation is usually used. This concept states that threshold stimulation is the lowest level of charge at which a muscle contraction can be elicited 50% of the time.

Figure 4: Experimental result showing electrode depth and threshold stimulation using swine model.

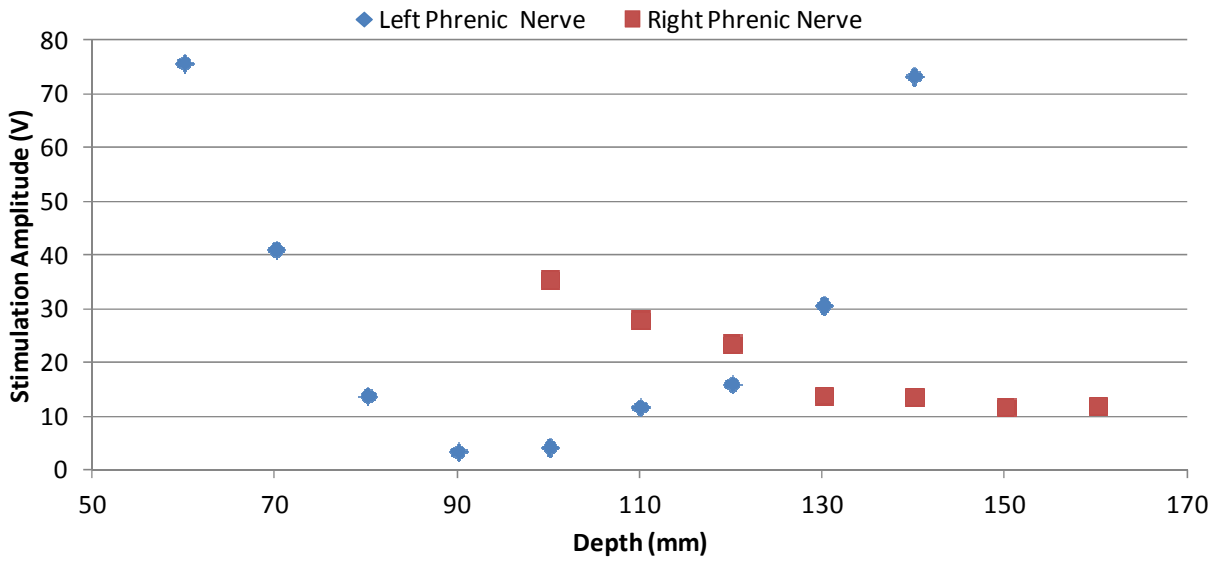

Note: Data from Acute Swine Experiment 5

With the left phrenic nerve running perpendicular to the left subclavian vein, placement of an electrode is optimized at a single site. Away from this location, stimulation efficiency quickly decreases as more electrical charge is required to produce the same stimulation; hence the parabolic shape seen on the left side of the graph. As the electrode is moved deeper and into the brachiocephalic vein and starts entering the superior vena cava, the stimulation efficiency quickly reaches an acceptable level for the right phrenic. Since the right phrenic runs alongside the superior vena cava, the stimulation efficiency remains nearly constant along the length of this vein. However, this blood vessel promptly leads to the heart where stimulation is not recommended and should be avoided as it may cause atrial fibrillation.

A parabolic relationship can also be expected when stimulating the nerves with the electrode at different orientations. Essentially, the efficiency of stimulation will decrease as the electrode area is rotated away from the orientation where the nerve can be found. A detailed theoretical analysis of this question can be found in a publication by Tang and Hoffer (2010).

1.1.4.1. Subclavian Catheterization

Although generally safe, subclavian vein catheterization for neurostimulation involves some non-negligible risks. Most risks are common to any catheter insertion, for instance sepsis

and thrombotic complications [Merrer et al., 2001], but one risk specific to the subclavian nerve cannulation is damage to the nerve, which can result in phrenic nerve palsy.

In a study looking at this issue, 42 adult cadavers were dissected in order to document the position of the phrenic nerve relative to the subclavian vein [Paraskevas et al., 2011]. In all but three cases, the left and right phrenic nerves were found crossing posterior to the subclavian vein. Two of the three exceptions had their left phrenic nerve cross anterior to the subclavian vein, while the last case saw the right phrenic run through the vein. Since ultrasonography does not provide any information as to the position of the phrenic nerve, it is therefore suggested that to minimize the risk of damaging the nerve when puncturing the vessel, the therapist should prefer an insertion site that is lateral to the jugulo-subclavian junction.

1.1.4.2. Nerve Mapping

With these narrow windows for optimal stimulation and the anatomical variability of patients, positioning the electrodes can become a difficult task. No currently available imaging method allows for easy identification and localization of the phrenic nerves and it is therefore necessary to use other clues for positioning the electrodes. The method used by the Neurokinesiology Lab involves advancing the electrode, stimulating at 1cm intervals and measuring the muscle response as an indicator of position. By looking for diaphragm activation visually and by recording intramuscular activation using electromyography (EMG) electrodes surgically implanted into the crural region of the diaphragm, it is possible to identify the threshold charge that elicits diaphragm contraction. This type of EMG is, however, too invasive for clinical application and needs to be replaced. In its current format, this mapping method achieves limited accuracy and traditionally involves more than 1 hour of testing to locate the ideal position for stimulating each nerve. Although this method can be suitable for research purposes, strategies need to be implemented to accelerate this part of the therapy.

Since most ICU patients under mechanical ventilation are under continuous infusion of sedatives to facilitate their ventilation [Kress et al., 2000 and Hansen-Flaschen et al., 1991], the duration of the mapping process is not predicted to be an inconvenience to the patient. Instead, to be an attractive therapy for clinicians to use, the mapping method needs to be streamlined to minimize the investment of time by the therapist. It is also believed that early placement of the catheter will best prevent the fast atrophy of the diaphragm muscle. Considering the research done by Levine et al, which states that diaphragm atrophy can be seen after as little as 18 to

69hours, delaying the onset of diaphragm pacing could have significant results on the outcome of the patient. The extent of this difference remains to be determined, since no data correlating the Lungpacer therapy and diaphragm atrophy is available at this time. Additionally, a lengthy positioning protocol could take time away from the tight schedule of therapists.

Other information emerging from conversations with therapists indicated that such a system would benefit from continuous lead position monitoring to maximize both safety and efficiency. With the therapy possibly extending over multiple days, many external events could affect the position of the leads. Therefore, the therapist should be alerted if the electrodes have moved from their optimal position.

2. Literature Review

With the phrenic nerve stimulation systems previously described either using a surgical approach or not disclosing their positioning method, a broader search for similar catheter positioning system is necessary. Positioning systems are becoming more common as robotic surgical methods are developed. Therefore, a significant amount of information is available about devices with capabilities comparable to what this project aims to create. Research projects from different corners of the world claim different methods of intravascular navigation while commercial solutions are also being offered by different medical companies. No disposable catheter positioning system was found commercially at this time. Nevertheless, it is pertinent to look for patents that may not be exploited at the moment but could limit the designs available for commercialisation.

2.1. Scientific Papers Review

Although no publications were found describing a disposable technology directly applicable to this issue, some research projects that are developing related technologies have been found. Arai et al. [2002] from Nagoya University developed a catheter-driving method for intravascular neurosurgery. Based on the mechanics of a mechanical pencil, their device was designed with safety, ease-of-sterilization and precision in mind. Even though this application requires a higher degree of accuracy, 10 to 100 times better than is needed for the Neurokinesiology Lab's application, the global concept is similar. Another device of the same type was developed at Kagawa University by Guo et al. [2007]. In this application, rollers are the main actuator of the system. Controlled by a stepping motor, the linear motion is said to be precise to 0.015 mm, which is also much more precise than required for our application. For their positional assessment, the system uses rollers coupled with an optical encoder while Arai et al. uses a laser displacement sensor. For control, each of these systems is a Master-Slave type using force feedback. Micro force sensors are used to provide feedback. For their devices, two sensors were used; one of the sensors measured force at the tip of the catheter, while the

other measured total force, representing the insertion force that a doctor would feel if moving the catheter by hand.

With the travel of these leads being around 0.5 meters and targeting small cerebral vessels, using force sensors appears critical. By relying on actuators for advancing the leads, including a force sensor becomes an essential aspect of the safety of such devices. The necessary travel and size of the vessels involved in endovascular phrenic nerve allows for greater safety margins than cerebral vessels, since the subclavian vein diameter is more than 10 fold larger. Therefore, the safety margin of placing an electrode less than 15cm from the insertion in such a large vessel is much larger than in the cerebral intervention counterparts.

2.2. Field Review

Even though many laboratories are developing methods and technologies for actuating and sensing the position of intravascular leads, few commercial products can be found. Systems available for locating a device's tip in a vessel rely mostly on imaging technologies. Some systems also make use of radioactive components to track the catheter tip in 3 dimensions. However, these systems require the use of large equipment independent from their system. The only product found which achieves positioning of a central catheter using an entirely self-contained system is the *Vasonova Vascular Positioning System* [Naylor et al, 2007].

2.2.1. Hansen Medical

The Sensei X Robotic Catheter System is a next-generation navigation system offered by Hansen Medical for complex cardiac arrhythmia procedures. The system keeps track of a catheter in 3 dimensions, and allows the user to control the movement of the catheter in 3 dimensions. To accomplish these complex tasks, the system relies on a series of proprietary technologies, amongst them: a robotic catheter with 6 degrees of freedom, a control stick with force-feedback, a remote controlled catheter driver and a visualization system to provide guidance. This visualization module uses MRI or CT scan slice data in order to reconstruct a tridimensional model of the heart and vasculature of interest. With each module integrated into the system, the therapist is able to manoeuver the intravascular device from a multifunction station.

Figure 5: Promotional picture of the Sensei X Robotic Catheter System

Note: Picture from hansenmedical.com

Considering that this system relies on an imaging system and multiple other components, it can be assumed that its acquisition requires large funds and dedicated space. Since its purposed is to navigate within the heart, its positioning system is much more complicated to what would be necessary to keep track of a catheter in a vein. However, Hansen Medical is one of the key players in catheter navigation systems having already announced two upcoming products which should extend the capabilities of the Sensei system.

2.2.2. Vasonova VPS

The Vasonova system offers a technology used for positioning a central catheter accurately in the lower portion of the superior vena cava. The purpose of this system is to eliminate the need for X-Ray imaging to position central lines. To achieve this goal, the navigation system relies on a catheter tip fitted with a Doppler ultrasound and an ECG electrode. The ultrasound information is used to determined blood flow around the catheter tip. It uses this information to determine if the catheter is going in the right direction, which should always be with the flow, and also to determine if the catheter tip comes into contact with the vessel wall, in which case the flow would be null. Meanwhile, the ECG electrode is used to sense the proximity to the heart. With this information the catheter can then be navigated to the lower third of the superior vena cava where it will be optimally placed for drug delivery.

Although appropriate in this context, this positioning system does not give any information about position in the general reference frame. However, the strategy of using ECG signals as a measure of proximity to the heart could potentially be used as a way to keep an electrode from getting too close to the right atria.

2.3. Prior Art

As important as what is already being used in the field and what is being developed in research labs is the technology whose rights have been reserved in the form of a patent. Although a multitude of patents relate to position tracking for intravascular devices, only a few very relevant patents will be summarized here. The patents in question are titled “Locating a catheter tip using a tracked guide” and “Therapeutic catheter with displacement sensing transducer”.

Both documents precede the start of this project. At the time of the redaction of this text, both documents were still at the application stage. Further inquiry on their respective statuses shows the following information.

Table 1: Prior Art Status

Therapeutic catheter with displacement sensing transducer (US2008/0140006)	
11-08-2010	On Appeal -- Awaiting Decision by the Board of Appeals
08-17-2009	Final Rejection
Locating a catheter tip using a tracked guide (US2008/0262473)	
11-20-2011	Abandonned. for Failure to Respond to O. A.
04-25-2011	Non-Final Rejection

2.3.1. Therapeutic catheter with displacement sensing transducer (US2008/0140006)

In this patent application filed by Boston Scientific, the technology described is a catheter fitted with a position sensor to track an element (which can be an electrode) within a housing. The application describes multiple methods used to track this *element* relative to the housing.

One of the methods described involves using an induction coil surrounding the element as it is moved within a sheath-like housing. With a portion of the element made out of a ferromagnetic material, the inductance sensed by the coil is proportional to the amount of material within its coil. This phenomenon is then converted into a position measurement. Multiple variants of this concept are also described. Those variants use, for example, an element whose ferromagnetic properties and dimensions are made to influence the inductance sensed by the coil.

A second method described involves a resistive coil or strip instead of an induction coil. In this embodiment, the moving element is fitted with an additional part that makes contact with the resistive element as it moves in and out of the housing. This additional part can, for example, be a leaf spring. The circuit is then closed by measuring the voltage drop between the point of contact and one end of the resistive element. The resistance varies proportionally to the length of the resistor the electrical current goes through, thus a voltage drop proportional to the position can then be measured.

An important aspect of the technology described in this patent application, is that the sensing element is said to be at the distal end of a catheter. In this instance, the distal portion is said to be the end that provides therapy or the diagnostic. Therefore, to avoid infringement of this patent, the position sensing would need to happen away from the distal end of the catheter, for example at the end that sits outside of the body.

2.3.2. Locating a catheter tip using a tracked guide (US2008/0262473)

This patent application describes a method for determining the position of a *first object*, like a guidewire, relative to a *second object*, such as a catheter. Although the text is fairly cryptic and rarely uses the terms catheter and guidewire, it is legitimate to believe that the preferred embodiment of the inventor involved both elements. Therefore, for the sake of clarity the first and second objects mentioned in the patent will be referred to as a guidewire and catheter respectively. Although electrodes are never mentioned in the document, it can be assumed that the guidewire could be substituted with a lead electrode.

In essence, the application describes a method which involves determining the position of one guide wire and inferring the position of the catheter by sensing only linear displacement between both objects. Some of the described embodiments – not all –mention the need for

determining the position of one of the objects in the global reference frame in order to infer the position of the second one. The methods for determining the position of the object include sending or receiving an RF signal, or determining the position a magnet, radiopaque or radioactive component which is part of the guidewire or catheter.

Although describing a “method”, this application mentions multiple ways to keep track of displacement between two objects. One of the embodiments described uses CCD sensors which read a code printed onto the guidewire. Another method described for determining displacement uses “calibrated gears or wheels” which convert the object’s linear movement into a rotation which is easily registered by encoder technologies.

In summary, this patent application describes methods of keeping track of two elements relative to one another, whereas the need of this project is more oriented toward keeping track of a position relative to the body itself. Most methods described in this patent application involve costly equipment which this project aims to avoid.

3. Design Specifications and Constraints

Designing a position sensor for an intravascular electrode system involves taking into account the sensor and the electrode's lead, but also the patient, the therapist, and the environment. This chapter will establish the requirements of each of these elements in order to adequately satisfy all aspects of the problem.

3.1. Specifications

The design specifications of the sensor are goals that should be met and exceeded when possible.

3.1.1. Linear Travel

The sensor shall allow each electrode array to travel downstream and upstream in their respective section of the vasculature. Each electrode should have a minimum travel of 50mm around the expected position of its target nerve. Subsequent generations of the sensor should benefit from more knowledge of the anatomical variability in subjects, which may allow for a shorter travel.

The need for a travel of 50mm arises from a variety of factors. Firstly, many parameters can vary from one patient to the next. These variations are thought to include the proportions of the individual and the verticality of the left phrenic nerve course towards the diaphragm. The extent of this variability is hard to establish and is not present in the literature. However, since the left phrenic is known to run along the side of the neck on the scalenus anterior [Fell,1998], it is possible to extrapolate some level of variation from measurements of neck widths. According

to anthropometric data[3], variations in neck width span approximately 2cm between the 5th and 95th percentile of each sex. Therefore one can expect the distance between the two nerves to follow the same sort of variation. This statistic suggests that the left phrenic nerve position may vary by at least 1cm along the subclavian vein.

Secondly, the distance from the insertion point to the nerve may vary based on the nature of the insertion. For example, variations in insertion depth due to the patient's body shape or weight have been reported as approximately 1.5cm [Tripathi and Tripathi, 1995]. Additional variations can also come from the different methods of insertion used [Fragou et al, 2011] as well as specific safety guidelines [Paraskevas et al, 2011]. Ultrasound-guided cannulation and landmark based method are two types of techniques which can lead to different locations of the puncture site. The magnitude of such variation can be estimated at around a maximum of 2cm.

Since this iteration of the system aims to be used in a preliminary fashion and not as a commercial product, more liberty to map a wider region than may be necessary is desirable. The information available suggests that the position in which the nerves may be found can vary by 3 to 4cm based on the insertion site and patient specific factors. Therefore a minimal travel of 5cm is reasonable for this iteration.

3.1.2. Angular Travel

Each electrode is expected to have an optimal orientation; however, limited anatomical variability data doesn't provide convincing evidence for limiting the angular movement of electrodes. Therefore, each electrode shall be allowed to rotate on its axis to permit exploration during pre-clinical and clinical trials. However, the angular orientation need not be recorded by any automated way at this stage. A detailed explanation of this decision can be consulted in Appendix B.

[3] NASA, Man-system integration, Volume I, Section 3: Anthropometry and Biomechanics

3.1.3. Linear Position Accuracy

To understand the desired level of repeatability and accuracy, one must consider the mapping procedure currently used. To find the optimal position for stimulation, threshold charge measurements were taken at 1cm increments. Each position is then characterized by a threshold level. When the lowest threshold is found, the user then brings the lead back to that position. Therefore, for the system to perform its role efficiently, it is important that the system be repeatable so that the lead can be precisely brought back to a previously measured position. Therefore, the accuracy of the system can afford to be limited, as long as requirement for repeatability is respected.

However, a rule of thumb of metrology states the accuracy of a system should be 10 times more accurate than what it aims to measure[4]. Since the mapping method involves increments of 10mm, the necessary accuracy can be estimated at ±1mm.

3.1.4. Linear Position Repeatability

Using data collected during multiple pre-clinical experiments using a swine model, we were able to map nerve stimulation efficiency. The data from left phrenic nerve maps can therefore be useful in understanding the need for repeatability, since this nerve is known to cross the subclavian vein at a single location.

Using a parabolic line of best fit data subset from 5 different animal models[5], it is possible to extrapolate a theoretical "true minimum" as shown on Figure 6. For comparison purposes, each of these nerve maps can be normalized to a fraction of the lowest threshold and plotted on the same graph. A closer look at the apex of these trend lines (Figure 6b) shows the rate at which the threshold value diverges from the extrapolated minimum. In order to consistently reposition a lead to within ±10% of the minimum threshold (below the orange line of

[4] According to multiple sources, including the "Role of measurement and calibration in the manufacture of products for the global market, A guide for small and medium-sized enterprises" by United Nations Industrial Development Organization, Vienna, 2006.

[5] The lines of best fit are second order polynomial trends. Although their fit to the data is limited (R^2 = 0.9 ± 0.4), their use aims to highlight the divergence of threshold charge for the case of the left phrenic nerve.

Figure 6b), a repeatability better than ±3.8mm would be necessary. However, since these parabolic relationships represent an extrapolation of the data, and the different traces show a high level of variation, one would be wise to look at the parabola with the steepest slope. The trend line in question is the one based on the experiment labelled “Chronic 2b”, and suggests a minimal threshold region of ±2.9mm. A safety factor of 3 can therefore be applied to obtain a maximum repeatability of ±1.0mm

Figure 6: Left phrenic nerve efficiency maps centered and normalized as a function of the extrapolated minimum

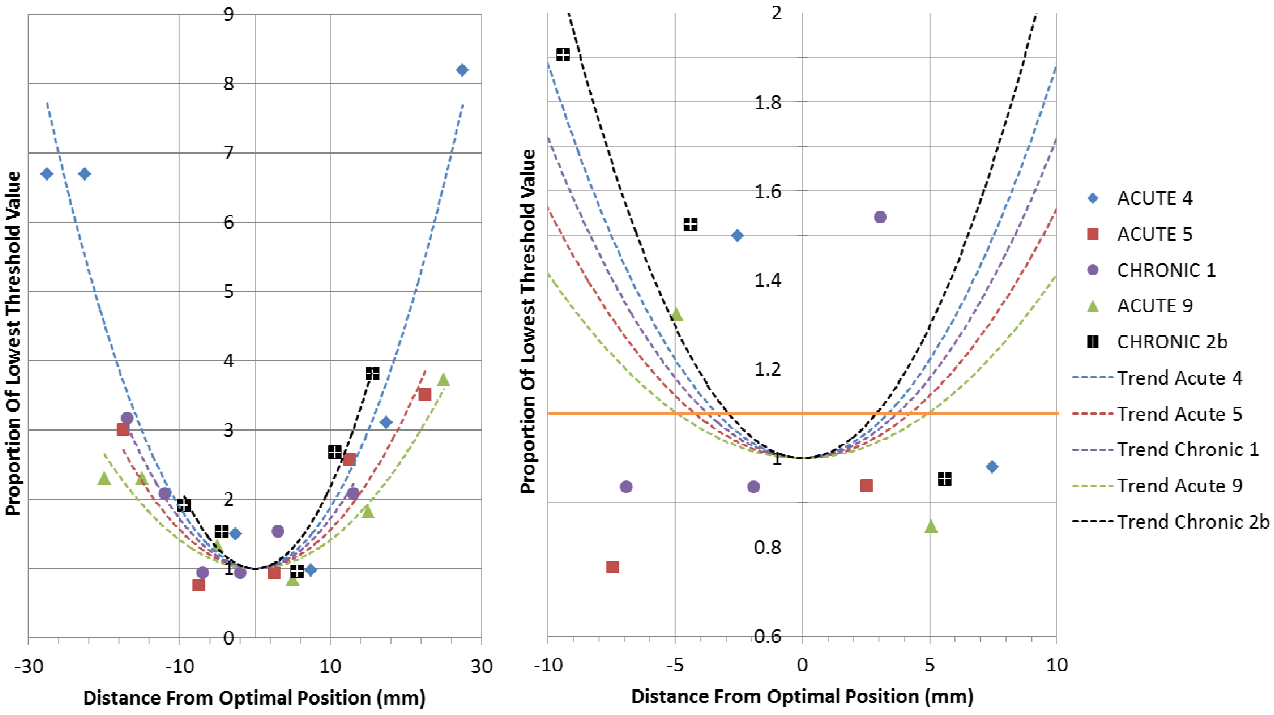

Note: A line of best fit was modeled after each of the data subset of the five animal models. Although the goodness of the fit of each curve is limited, each line of best fit is meant to illustrate the divergence of the threshold charge level from its minimum. Using the trend lines, it is possible to see that the data from the five animals shows different gradient as they diverge from their minimum. A level of 10% above the lowest threshold can be used to describe these curves represented by the solid orange line of Figure 6b. On average, the line of best fit crosses this 110% threshold value at ±3.8mm, and in the worst case, at ±2.9mm for the “Chronic 2b” data.

3.1.5. Push/Pull Force

The force required for movement of the leads once assembled with the sensing unit shall be minimal so that the therapist will still be able to feel the resistance of the electrodes as they

are moved within the blood vessel. In other words, the resistance offered by the sensing assembly should not mask the resistance of the vessel itself. In a study performed to determine the force required to cause a perforation in a swine atria using an ablation catheter [Perna et al, 2011], the average force reported was 175.8±60.4g (1.72±0.59N) while the lowest force that created a perforation was 77g(0.75N). However, the forces reported excluded the frictional forces caused along the length of the catheter. Also, although the structure studied was the right atrium and not the SVC or subclavian vein, the force required to cause damage to such vessel walls is likely of similar amplitude. Considering that the lowest amount of force found to cause perforation was 0.75N, it is imperative that the resistance induced by the assembly be lower than this value so the therapist is still able to distinguish this small, but potentially damaging force on the vessel wall. Additionally, the leads to be used in association with this system are being designed to avoid small areas of contact in order to make perforations less likely. Instead, the design shall spread the force over a larger area than would a catheter with a 2.5mm round-tip like the one used in the Perna study.

3.1.6. Fatigue

The sensor shall be able to perform at least 50 cycles and maintain the same level of performance. A regular instance of nerve mapping should involve, one scan of approximately the whole travel of the sensor, coming back to the optimal position, and potentially a few repositioning of the electrodes over the course of the therapy which can last up to three weeks. Therefore, during an entire therapy with a given patient, each sensor should not be put through its entire travel more than 2 to 3 times. By setting the minimum number of cycles for the system to withstand at 50, a safety factor of more than 10 is ensured.

3.2. Constraints

The viability of this project is greatly dependant on certain constraints that cannot be circumvented. For the sensor to be suitable for hospital use, it will have to fulfill all of the following criteria.

3.2.1. Intuitive control of electrodes

The position and orientation of the electrodes shall be modified using an intuitive method that does not require any training, and limits possible manipulation error. If instruments such as knobs or sliders are used, they shall be clearly identified with the electrode it controls.

3.2.2. Prolonged use

Considering that therapy will likely span from a few days to a couple of weeks depending on the patient, it is desirable to maintain electrodes at their optimal position throughout therapy. The sensor shall then allow measurements to be taken over a long time span. Although no equivalent catheter-based transvascular stimulation system is currently used in intensive care units, intensivists and other ICU staff have been informally consulted and asked to describe the challenges that might arise from the extended use of such an intravascular system. Elements highlighted by therapists include the need to move the patient from time to time, which may result in a shift in electrode position, which would then require repositioning. It was also mentioned that occasionally patients in ICU need to be imaged using magnetic resonance imaging (MRI). If the system is permanently associated with the catheter, it should also be compatible with MRI technology.

If the sensing unit is removable, then it should have the ability to be easily put back on the leads to make position measurements within the same reference frame. On the other hand, if the sensing assembly is not removable it should not be an inconvenience to the patient, or cause substantial discomfort.

3.2.3. Fixed reference frame

For positioning to be reproducible, the sensor shall be placed in a fixed reference frame. This reference frame will have to move with the patient so that the position of each lead is always measured from the perspective of the body. To achieve this, the sensors could potentially be sutured or taped to the skin, or be fixed at a known distance from the lead entry point into the body or another suitable reference.

3.2.4. Digital acquisition of position

To allow for future integration with a computerized control unit, the position data shall be digitized automatically. The sensor assembly shall therefore allow for the appropriate cabling or communication protocol (if wireless).

3.2.5. Maintain safety and functionality in a clinical setting

Under standard use, the sensors may be exposed to blood and other fluids. It is therefore essential that the system remain safe and functional when exposed to these conditions.

3.2.6. Allow sterilization

The sensing unit shall be compatible with conventional methods of packaging and sterilization. Those methods include steam, gas, and radiation sterilization. The method used should be compatible with the lead assembly.

3.3. Other Design Considerations

3.3.1. Lead Design

At the center of this project are the electrodes that need to be placed. These electrodes and their leads have their own limitations and interact with the design of the position sensor in various ways. Therefore, care has to be taken in designing the position sensor without limiting the electrode and vice versa.

3.3.2. Minimize environmental impact

Environmental impact shall be minimized as much as possible. To accomplish this, the materials and components shall be easily recyclable. Electronics certified as RoHS compliant

shall be preferred to competitors[6]. Additionally, if the sensing unit is disposable, its volume shall be kept to a minimum as to not create useless waste.

[6] RoHS stands for Restriction of Hazardous Substances Directive. Therefore a device which is RoHS compliant has been tested for substances harmful to the environment.

4. Design Methodology

4.1 Design Method

The sensing unit was designed using a computer assisted design software called *SolidWorks* due to its accessibility to students. *Solidworks* is also one of the most used CAD software in the industry. Most fabrication shops are therefore well equipped to interpret 3D drawings made with this software.

4.2 Testing Method

To validate concepts and prototypes, tests were performed both in vitro and in a pre-clinical setting. However, most of the validation was performed using bench tests. Using a mock-lead, the following tests were performed:

- Travel Test
- Accuracy/Repeatability Test
- Movement Resistance Test
- Fatigue Test

True validation is not possible without using the device in the setting it was designed for. However, since testing in humans was not accessible at this time, the alternative was to use the sensor during preclinical experiments in an animal model. In this setting, the global usability can be tested as well as its behavior outside of a controlled environment (for instance, where blood and other fluids can interfere with the functionality).

4.2.1. Travel Test

This test was used to determine the travel allowed by the prototype for both linear movement which was registered by the sensor, and the rotational movement which was allowed by the assembly.

This test used Mastercraft electronic caliper with digital display. The tool had a resolution of 0.01mm and an accuracy of 0.02mm.

4.2.1.1. Preparation

1. Assemble the prototype.

4.2.1.2. Execution

1. Start the data acquisition system.
2. Couple the lead to a digital caliper in the way shown in Figure 7.
3. Move the lead to its most proximal position and note the position.
4. Move the lead to its most distal position and note the position.
5. Rotate the lead, and note the largest span of movement allowed by the assembly.
6. Record the rotational travel allowed by the unit.
7. Stop the data acquisition system.

4.2.1.3. Data Processing

1. Calculate linear travel as the difference between the positions measured at step 4 and 3.
    a. The continuous travel should only include positions where the force required for moving the lead is estimated as continuous. Major variations in push/pull force, should be used to determine the start or the end of travel.
    b. Use the data acquisition system to indicate where the bead is in contact with the sensor. The lack of contact between the sensor and the bead can be used to determine the start or the end of travel.
2. Measure rotational span using a protractor to measure the movement of a marking on the side of the lead.

4.2.2. Accuracy/Repeatability Test

This test is used to determine the measurement accuracy and repeatability of the system. The protocol can be repeated for multiple units, or sensors, and the results can then be averaged over a population of same prototypes.

4.2.2.1. Preparation

1. Assemble the prototype.
2. Calibrate the sensor.
    a. Measure 5 to 10 evenly spaced positions.
    b. Calculate the relationship between the position and the sensor signal.
3. Determine 5 randomly spaced targets that represent the full linear travel of the prototype.

4.2.2.2. Execution

1. Start the data acquisition system.
2. Couple the lead to a digital caliper in the way shown in Figure 7, using the same caliper described for the travel test.

3. Move the lead to each of the predefined locations in succession.
4. Repeat 10 times.
5. Stop the data acquisition system.

Figure 7: Accuracy/repeatability test setup

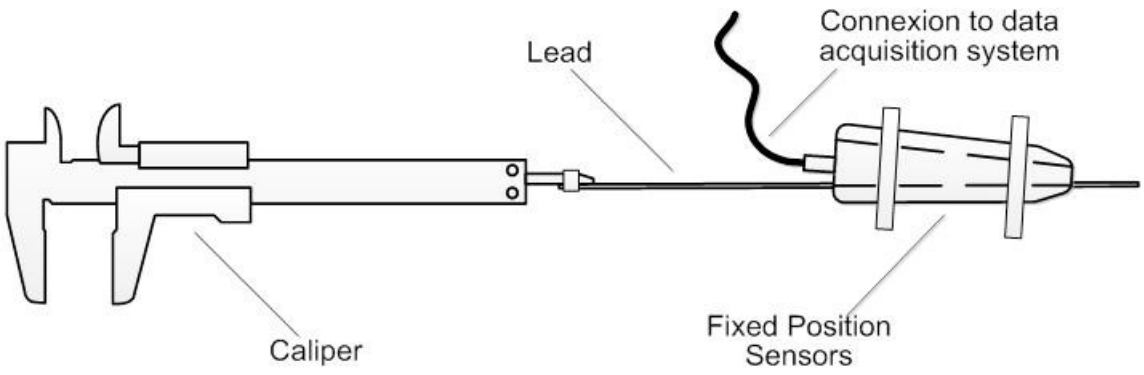

4.2.2.3. Data Processing

1. Identify the voltage value of each measurement, and apply calibration.
2. Calculate the difference between each measurement and its target.
    a. The average difference is the accuracy of the unit.
3. Calculate the standard deviation of all measurements for each target.
    a. The average standard deviation is the repeatability of the unit.

4.2.3. Movement Resistance Test

This test aims to quantify the force required to move a lead up and down the positioning system. This test used a MARK-10 force gauge model M3-2. The resolution of the force gauge was 0.01N.

4.2.3.1. Preparation

1. Assemble the prototype.
    a. The prototype does not need to be connected to the data acquisition system.

4.2.3.2. Execution

1. Fix the force gauge to the end of the lead.
2. Pull in the axis of the lead, taking the lead through its entire travel, without reaching the end.
3. Record the peak tension force.
4. Repeat 5 times.
5. Fix the force gauge to the other end of the lead, and repeat steps 2 -4.

Figure 8: Movement resistance test setup

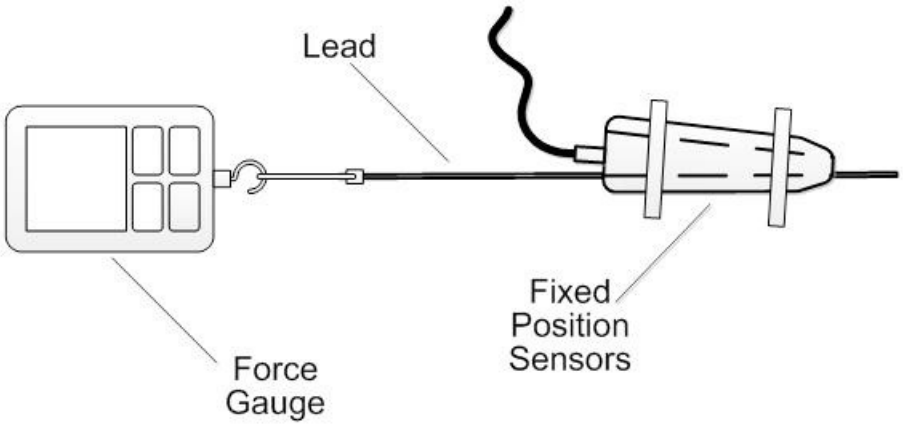

4.2.3.3. Data Processing

1. Calculate the average of the measurements of each force direction.
2. Calculate the standard deviation of each average.

4.2.4. Fatigue Test

This test aims to qualify the behaviour of the prototype after multiple cycles.

4.2.4.1. Preparation

1. Perform Accuracy/Repeatability Test.
2. Perform Movement Resistance Test.

4.2.4.2. Execution

1. Take the sensor through its entire travel and back.
2. Repeat Step 1 fifty times.
3. Perform Accuracy/Repeatability Test.
    a. Calibration does not need to be performed again. The initial calibration shall be used to compare results.
4. Perform Movement Resistance Test.

4.2.4.3. Data Processing

1. Compare the results of Accuracy/Repeatability from before and after cycling.
    a. Check for significant differences between the results before and after the fatigue test.

5. Sensor Choice

The most important part of this project was to find or create an appropriate sensor to keep track of position, and then couple it to the element for tracking. A broad search for linear position transducers was therefore performed. Throughout this search, multiple sketches were made to explore how different sensors would integrate into this system. Many sensor types were eliminated due to their size, price or simply the complexity involved in coupling them to the leads. After outlining the major types of sensors that were considered for this system, the sensor that was ultimately chosen will be described in detail.

5.1. Main Sensor Types

After all the different types of sensors were explored, some sensor families were eventually shortlisted and considered more carefully. Amongst them were optical sensors, rotary encoders, Hall-effect sensors, and a sub-family of linear potentiometers, membrane potentiometers.

5.1.1. Optical sensors

Optical sensors come in a variety of different types. The most interesting types explored for this project were CCD sensors, and a subset of the same family, infrared reflective sensors. Although similar at first sight, both technologies offer advantages and disadvantages that differ greatly.

Charge-couple devices (CCD) are a technology widely used today in products such as cameras and computer mice. Most (not all) CCD sensors are used to capture images. To do so, the CCD sensor is covered by an array of capacitive photoactive elements that absorbs light and converts it to an electric charge. To process the image, each element passes its charge to its neighbour while the last element of each line passes its charge to an amplifier, which, in turn, converts it into a voltage that can be processed. They come in various sizes, which are usually proportional to their resolution, but can also differ in shape depending on their application.

When serving as a position sensor, CCD arrays are used for taking repetitive images of a surface. To allow for a proper visualization of the surface, the sensors are usually coupled with a light source to illuminate the surface. The images are then compared sequentially to calculate the relative movement of pixels between each pair of images. Assuming a certain distance between the surface and the sensor, number of pixels can then be used to determine movement. This very common concept can be found in most modern computer mice.

Despite their frequent use and low cost, such sensors are not recommended for positional systems that work under open loop conditions. The reason for this is that computer mice don't need a particular level of accuracy, or even repeatability, because of the visual feedback provided by a cursor on a screen. In this form, any of the sensor's imprecision can be easily corrected by the user as he sees the cursor move closer to the target. Therefore, manufacturers of mouse sensors do not rate their products for specific positional accuracy and hysteresis. Instead, manufacturers traditionally aim to seduce their customers by offering an acceptable resolution while minimizing the price of their sensors.

Because of this lack of documentation on the performance of mouse sensors, a simple test bench was produced to estimate their level of precision. To do this, a sensor was used directly from a working mouse. The mouse was fixed to a flat surface where a small piece of plastic could be slipped linearly under the mouse sensor while maintaining contact with the mouse's underside. By doing so, the distance between the sensor and the object moved was ensured to be the one the mouse was designed for. An illustration of the test bench is provided in Figure 9. The sensor's output was then intercepted and recorded by a computer program. Using the plastic strip, the sensor's output was calibrated and converted to displacement measurements. The sensor's output was then tested by using various plastic strips with various surface finishes from smooth to rough and patterned with pen drawn lines.

Although accuracy of the sensory was sometimes within 1mm, its hysteresis was unpredictable. For a movement of about 10cm one way and then back to the start position, the difference between the initial and final position calculated by the software would vary by about 3mm on average.

Figure 9: Mouse sensor characterization setup

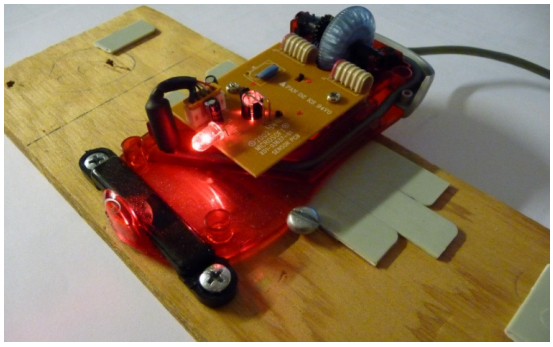

Through discussions with a mouse sensor sales representative, the poor result in hysteresis was attributed to the determination of individual displacement measurements between pairs of images. By averaging the different pixel's displacement for each individual measurement, the system's calculations can differ slightly for each passage over the same surface. Over the course of a few centimeters' travel, these differences can add up to a substantial distance. Therefore such low-cost mouse "cameras" cannot be integrated into a positioning system for a medical device in their current form. However, a simplification of the same technology can solve part of this hysteresis problem and allow a much greater reliability.

By using a similar camera-based system to look for a known feature, some optical sensors are often used to measure distances in open loop systems. One of these sensor families is infrared reflective sensors. As their name states, those sensors use infrared light reflections to determine position. By shining the light on a code strip of alternating reflecting and non-reflecting surfaces, the sensor detects the reflection of its own light and converts it to a relative displacement.

Figure 10: AEDR-8400 sensor, a low-cost reflective encoder

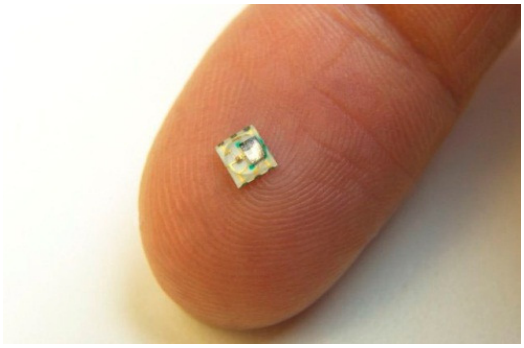

Note: Picture from Avago Technologies AEDR-8400 series datasheet.

Offered in different sizes and precisions, those sensors are also very affordable, selling usually for between $2 -10. For example, the AEDR-8400 sensor series of *Avago Technologies,* shown on Figure 10, offers a maximal resolution of 80microns for $5 while being no larger than 9mm^2. However, multiple inconveniences exist with such optical sensors. The first inconvenience is the positioning precision necessary for reading a code strip. In other words, the sensor has to be placed with a very specific distance and alignment relative to the reflective code strip in order to reliably detect its movement. Secondly, multiple restrictions limit the shape of the code strip to be used. More specifically, the strips have to be at least 1.8mm wide in order to ensure proper reflection of the beam of infrared light back to the sensing element of the sensor. However, to apply this sensor technology to an intravascular lead positioning system, reflective markings would have to be printed onto the surface of the lead. As shown in Figure 11, using a lead of about 1mm in diameter, most of the rays of light would be reflected away from the sensor instead of back to the sensing element. Using such a sensor would require going beyond the parameters recommended by the manufacturer.

Figure 11: Illustration of the infrared sensor used to detect a lead's displacement.

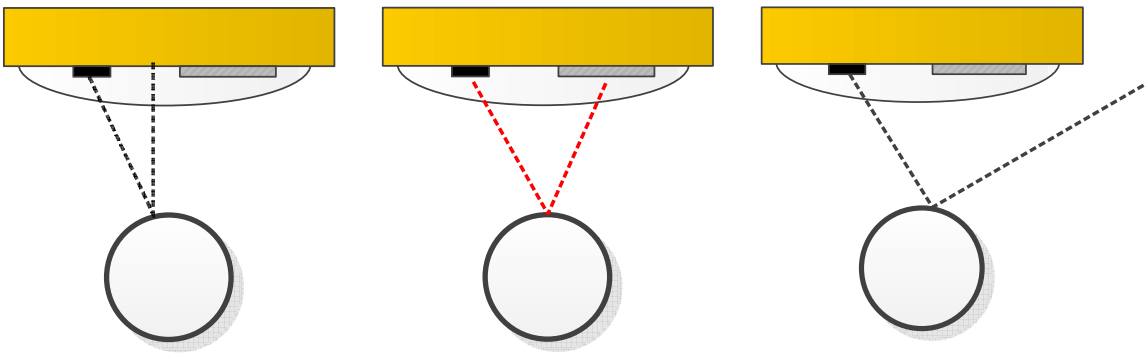

Note: The three images show that only a fraction of the light would be reflected into the sensing element of the sensor because of the curve of the surface.

5.1.2. Rotary encoders

Rotary encoders are amongst the oldest and most standard technology used for motion control in electromechanical systems. Also called shaft encoders, those sensors describe movement by detecting angular movement of a shaft. One of the common principles of operation of such encoders uses a light, a light detector and a disc with holes that is mounted onto the shaft. As the shaft rotates, the holes in the disc alternately let light reach the detector.

The detection of light is then converted into a voltage, which can then be correlated to a relative angular position. Multiple variations of this simple concept exist to improve resolution and add information about direction of rotation.

Encoders of this kind are often used to derive linear motion because they are easily assembled onto an electrical motor. However, they can also be used to deduce linear displacement if used in a roller system. In the case of an intravascular lead, as it's been shown before in the case of Guo et al., rollers can also be used to actuate a lead. However, in this context, the roller speed is controlled, and can be set appropriately to minimize slippage between the rollers and the lead. In the case of our system, where the lead is controlled manually, the lead would run the risk of slipping against the roller, which would induce poor repeatability. Also, due to the nature of their concept and the need to translate the linear movement into rotation, such encoders can be relatively bulky.

5.1.3. Hall-effect sensors

Hall-effect sensors respond to the presence and direction of a magnetic field. Used alone, a single sensor can only measure the magnitude of a magnetic field in one direction. However, if used in conjunction with other sensors, a tridimensional position can be measured.

Figure 12: Spatial representation of the working principle of Hall-effect sensors.

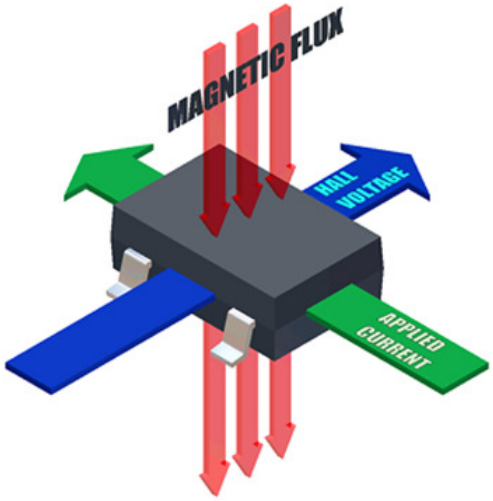

Note: Picture from http://www.ecnmag.com/uploadedImages/Ecn/Articles/ec94sz101a(1).jpg

The principle behind the "Hall-effect" is the following: by placing an electrical conductor carrying a current within a magnetic field, a voltage difference will be generated in the direction

perpendicular to the current and the field (Equation 1). In other words, the potential difference created by a magnetic field can be used to calculate the distance between a magnet and the transducer. By using a calibrated magnetic element as the tracked object and setting the current in the conductor to a known value, the position of the magnet can be extrapolated from the voltage generated by the hall-effect sensor.

$$V_H \propto I \times B \qquad \text{(Equation 1)}$$

To be used in a practically setting, a few controls have to be put in place. Typically, the sensor also has to be temperature regulated to avoid any drift in the signal. Also, the sensor has to be supplied with a regulated voltage, and its output has to be amplified via a differential amplifier. These measures allow the current going through the conductor to be held constant. With these control elements, only the magnetic field's effects are reflected in the measured potential.

This type of sensor offers the advantage of providing position measurements without any contact between the sensor and tracked element. To do this, a magnetic element would have to be added to each lead. Geometrical constraints on the design of the leads would greatly limit the size of such magnetic elements. Hall-effect sensors are also subject to the effects of magnetic fields that may emanate from other electrical devices. Considering that ICU patients are commonly in an environment where vital monitors can be found as well as mechanical ventilators, and various other devices that can potentially generate electromagnetic noise, the use of a hall-effect sensor could be problematic. Additionally, proximity to a magnetic resonance imaging system could introduce a great deal of interference to such sensors.

5.1.4. Linear Potentiometers

Potentiometers are electrical components that serve as adjustable voltage dividers. A subset of this large group is linear potentiometers. Even this subset comes in numerable shapes and sizes. Some of the embodiments of this technology come in the form of telescopic cylinders (Figure 13*a*), sliders in a track (*b*), or as collars on instrumented shafts (*c*). However, the size and mechanical complexity of those sensors do not lend itself to a disposable positioning system such as the one being developed here.

Figure 13: Examples of linear potentiometers[7]

(a) **(b)** **(c)**

Membrane potentiometers are another type of linear potentiometer which lend themselves more readily to an application of this type. Membrane potentiometers are thin sensors that use pressure along a conductive membrane to produce a variable resistance. When the conductive membrane is deformed by a punctual pressure, it shorts a resistance trace. The position of the contact along the trace therefore determines the distance travelled by the electrical current in the resistive trace, creating a voltage drop proportional to the position of the point of contact. Figure 14 shows this principle by showing a sectional view of a membrane potentiometer. To use such sensors appropriately, their active region has to be placed on a flat surface. Bending of the active region could otherwise create a contact between the two membranes, which would produce an erroneous position signal.

[7] Pictures are respectively from:

(1) http://www.precisionsales.com/potentiometers/linear-motion/images/LCPL-linear-potentiometers.jpg

(2) http://www.tme-france.com/en/ref/86_1.jpg

(3) http://www.gefran.com/image_resized.aspx?method=F&w=240&h=260&cp=1&src=/images/resources/prodotti//cf650723-9bc0-4aa6-bd02-26445faf3d84_PMA.jpg

Figure 14: Working principle of membrane potentiometers

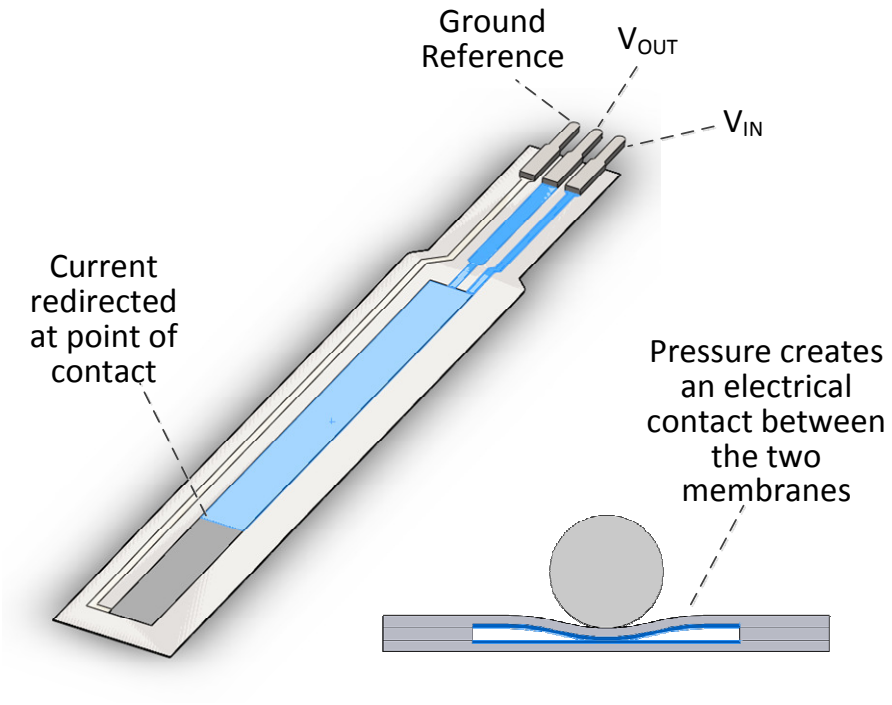

Membrane potentiometers offer limited accuracy with a linearity error of around 2%. However this error can be lowered to about 0.5% using certain materials. Additionally, when used in a fixed reference frame, these sensors offer absolute position measurements. Therefore, repeatability of measurements can be expected to remain under the linearity error. A probable inconvenient of such sensors can be expected to be a short lifetime due to wear and tear of such thin polymers, however manufacturers still advertise lifetimes of about one million cycles. A risk that still remains is the effect of storing this type of sensor with a wiper in the same position for an extended period of time, as a plastic deformation of the membranes could potentially occur.

5.2. Final Sensor Choice

After considering these families of sensors and their potential application in an intravascular positioning system, membrane potentiometers appear to be more promising than any other type of sensor available. This type of linear potentiometer offers numerous advantages.

The first reason for using membrane potentiometers is the simplicity of its signal acquisition and processing. By being a simple voltage divider, these linear potentiometers offer an output that is easy to control, to condition, and to debug in case of a malfunction. Unlike rotary encoders that rely on timing of different signals to compute direction of movement and position, membrane potentiometers are absolute position sensors that produce a voltage proportional to a position.

Secondly, because the sensor's travel is defined by its geometry, manufacturers are readily open to designing sensors with customized dimensions for a reasonable price. As a result, a sensor can be made to the precise specifications of this project once the variability of electrode phrenic nerve position has been better determined. Another possibility offered by these customized sensors, would be have sensors of different lengths for different patient populations in order to minimize sensor size.

Thirdly, on the topic of environmental impact, some embodiments of this technology have already received a RoHS certification. Meanwhile, those that do not have the certification can be expected to obtain it shortly. Considering that their functionality doesn't rely on any of the restricted materials listed by the RoHS certification, it should be assumed that none of them contain the proscribed materials.

Additionally, since this technology is not exclusively associated with one manufacturer, many different geometrical configurations are available off the shelf. Elements that vary between versions are the length of the active region, the thickness of the sensor, the resistance span, and responsiveness to contact. Prices for these sensors usually range between $15 – 20.

Table 2: Comparison of different membrane potentiometer products

Sensor Name	*FlexiPot*	*SoftPot*	*SensoFoil*
Manufacturer	Tekscan	SpectraSymbol	Hoffmann&Krippner
Active Travel (mm)	63.5	50	82
Sensor Length (mm)	91.3	65.86	100
Active Width (mm)	4.3	7.1	6
Width (mm)	11.6	20.3	22
Thickness (mm)	0.208	0.51	0.7
Resistance (kOhm)	10	10	2.5
Resistance Tolerance	N/A	±20%	± 30%
Linearity	<±2%	3%	2%
Repeatability	<±1% of Full Scale	Infinite	0.5mm
Material	Polyester (Mylar)	N/A	PET foil
Price ($)	14.63	12.95	18.12
RoHS	✓	✓	X

*The information in this table comes from product specification sheets and other official sources.

Out of the many versions of membrane potentiometers available, Tekscan's *FlexiPot* sensor appeared to be the most adequate. Compared with its two competitors, the FlexiPot is much more compact as its dimensions outside of the sensing region are much smaller. Linearity advertised by Tekscan is also better than the competition. However, variation of the sensor's resistance is not mentioned in their datasheets but it would be reasonable to assume variability between 10 and 30%. In this case, like its competitors, a calibration would likely be necessary for each sensor.

SpectraSymbol's SoftPot also showed good potential. Just like the FlexiPot, it is certified as RoHS. Therefore, both the FlexiPot and SoftPot were purchased and compared qualitatively. The result of the comparison was that the FlexiPot was much more responsive than its competitor. The FlexiPot was then chosen for tracking of the linear position of the lead. A picture of the sensor can be seen in the following figure.

Figure 15: FlexiPot sensor from Tekscan

Note: Picture from tekscan.com

To provide additional design input, and clarify the specifications which have been reported, more tests were carried out.

5.3. FlexiPot Performance Testing

To validate the choice of the sensor selected to track electrode depths, a few characterization tests were performed. These tests aimed to give a practical understanding of the product's specification and qualify properties which were not covered by the specifications. The first test looked for the sensor's constant output over an extended period of time. The second test aimed to qualify the sensor's behaviour when exposed to fluids.

5.3.1. Signal Temporal Variation

With medical products often being left on hospital shelves for weeks or months, it is important for them to retain their properties and remain calibrated. Accelerated aging tests are typically used to verify the behaviour of a sensor over an extended period of time, however, those experiment require temperature regulated testing setups over extended periods of time. By increasing the temperature by increments of 10°C above the temperature at which the device is used, it is believed that all aging processes will be accelerated two-fold for each 10°C increments [Lambert and Tang, 2000]. The typical temperature accuracy of such apparatus is around 0.5°C over temperature of 40 to 60°C. With this equipment being unavailable at this time, the test was performed at ambient temperature instead.

To perform this test, three *Tekscan FlexiPot* linear potentiometers were used. All three sensors were fixed to a solid surface with adhesive for the duration of the test. Lines were traced with a felt maker at three positions on each sensor to determine the location at which each measurement will be taken. The sensors were supplied with 5V for the duration of each measurement. Measurements were taken each 2 to 3 days for a total duration of 21 days. To perform each measurement, a round-tip tool was used to manually press down on the sensor

strips at the position where lines were traced. The signal was acquired using an oscilloscope averaging the signal over 2 seconds

The following graphs show the variation of each measurement as a percentage difference from the average result of each position. The largest single variation from baseline is 0.048V which represents a distance of 0.66mm. No significant trend was observed in any of the traces. Table 3 summarizes the variation in the data.

Figure 16: Signal variation graphs for 21 days of testing

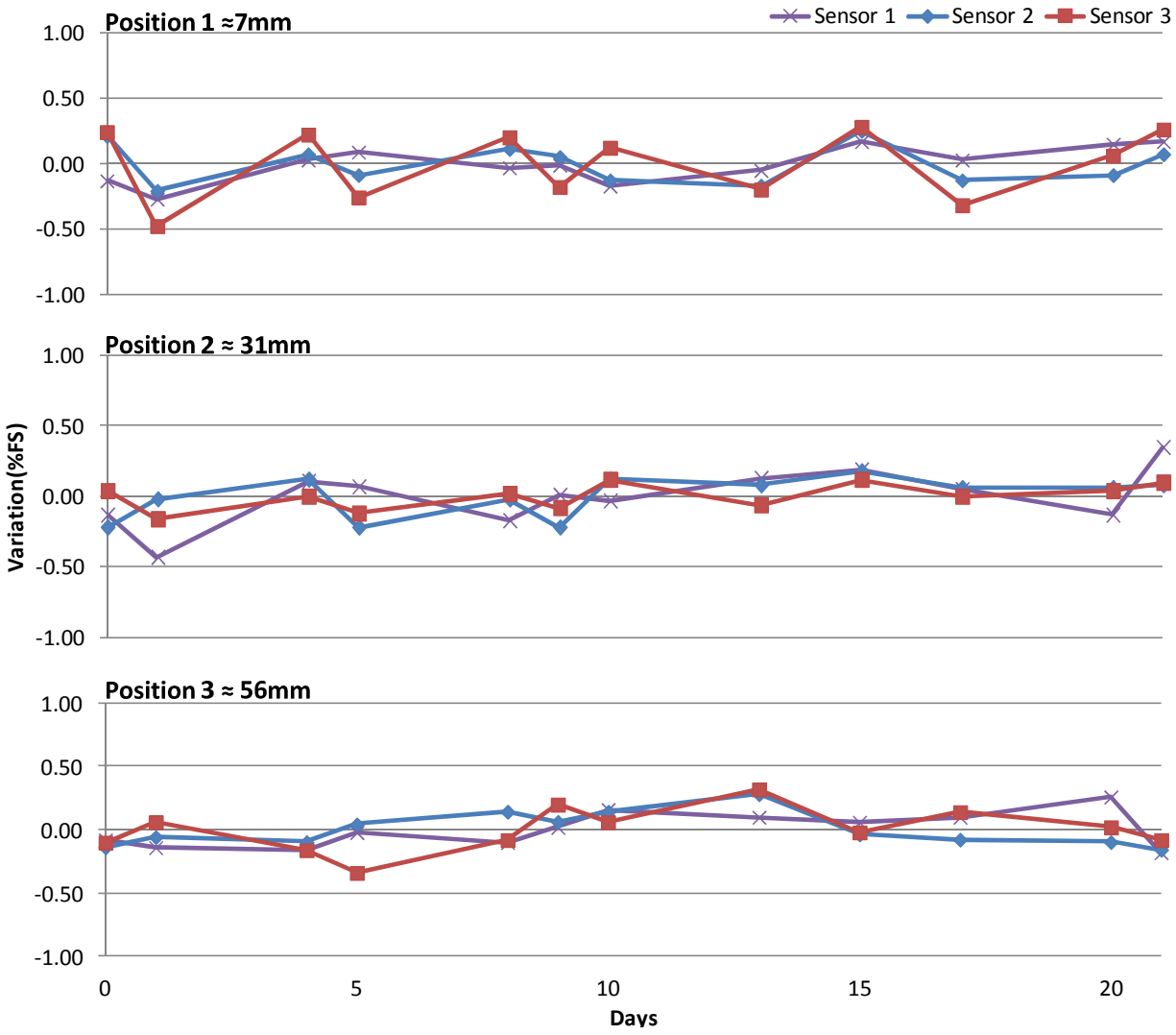

No trend was detected in each of the traces. The maximal variation observed throughout the test was within product specifications for repeatability (1% of full scale). Additionally,

variations are expected to come from the method used for inducing pressure on the sensor. Applying pressure manually using a hand-held tool could potentially have induced an error of ±0.5mm. Another factor of error comes from the felt marker used to trace target lines which gave targets of about 1.5mm in width.

5.3.2. Resistance to fluids

With the sensor potentially being exposed to variable amounts of blood and other fluids, qualifying the behaviour of the sensor under such conditions is essential. Although many strategies can be implemented to limit or even avoid exposure to fluids, the most severe exposure was tested by submerging the sensors in saline solution.

To perform this test, two *Tekscan FlexiPot* linear potentiometers were used in different conditions. One sensor was only immersed up to and excluding its electrical contacts while the other sensor was immersed entirely in saline solution. Lines were traced with a felt maker at two positions on each sensor to determine the location at which each measurement will be taken. The sensors were supplied with 5V for the duration of each measurement. After a baseline measurement on day 0, measurements were taken at growing intervals (5min, 20min, 1h, 3h, 24h, 3 days, and 7 days) until the component's failure to produce satisfactory results. To perform each measurement, a round-tip tool was used to manually press down on the sensor strips at the position where lines were traced. The signal was acquired using an oscilloscope averaging (V_{avg}) the signal over 2 seconds and calculation the peak to peak amplitude of the signal (V_{pp}). The use of an oscilloscope as the measurement tool provided a lower resolution than the data acquisition system typically used to measure the signal of the linear potentiometer. However, this method was chosen in order to be able to visualize any potential fluctuation and drifts in the signal.

Table 3: Fluid resistance results for a sensor with the electrical contacts not submerged

	Contacts not submerged		Contacts submerged	
	3.0cm	**6.0cm**	**3.0cm**	**6.0cm**
	V_{avg} (V)	**V_{avg} (V)**	**V_{avg} (V)**	**V_{avg} (V)**
Baseline	2.67	4.78	2.67	4.78
5min	2.67	4.78	2.67	4.78
20min	2.68	4.80	2.68	4.80
60min	2.67	4.78	2.67	4.78
3h	2.68	4.79	2.68	4.79
24h	2.68	4.75	Drifting	Drifting
3days	2.67	4.78	-	-
7days	Drifting	Drifting	-	-

Failure was observed after 7 days for the sensor whose contacts were not submerged. The signal was seen drifting significantly on the 7th day. It is possible that the drift was caused by water moving between the films and displacing the shortest route that the current had to take. However, by using saline solution, it was possible to observe that the contacts were covered with precipitated salt. Therefore it can be theorized that some capillary effect took place and carried fluid up to the contact where it entered infiltrated the sensor, and caused failure.

The sensor which was submerged entirely in water failed after 24 hours. The interface between the electrical contacts and the potentiometer's membrane being exposed to fluids, it is likely that fluids infiltrated the sensor through this path.

After failure, water could be seen between the sensor's membranes, most likely causing a short between the sensor's components. After approximately 2 months, the sensors were tested again and their performance was restored back to their original spec. The water that had entered the sensor probably evaporated.

This test shows that to minimize the chances of fluids causing failure in the sensor, the electrical contacts should most likely be encapsulated or otherwise isolated. Considering the electrodes should only ever be used for durations shorter than 30 days, silicone encapsulation should slow the progress of fluid long enough to postpone failure during the time where the sensor is used. Additionally, blood is more viscous than water and coagulation should also make blood less invasive than saline solution.

5.3.3. Resistance tolerance

As is shown in Table 2, *Tekscan* does not provide a value for the resistance tolerance of their *FlexiPot* membrane potentiometer. Although it is not possible to know the exact method used by manufacturers to calculate the "resistance tolerance" of their potentiometers, using statistics it is possible to infer the range of the resistance tolerance.

The total resistance of 8 units was measured. The results were then compiled and a confidence interval was extrapolated using a student t-test for small samples. The confidence level was set at 99.9%. The following table summarises the results of this simple study.

Table 4: FlexiPot resistance test results

Average (kΩ)	Standard Deviation (kΩ)	99.9% Confidence Interval (kΩ)	Resistance Variation as a Proportion of Average (%)
9.71	0.26	[8.8, 10.6]	±14.7

To compare the results with the resistance tolerance of other membrane potentiometers, one has to look for the proportion of the total resistance included in the confidence interval. Although this method cannot be guaranteed to be the same used by manufacturers, the value obtained is comparable to the values of other manufacturers (Flexipot: ±14.7%, Softpot: ±20%, SensoFoil: ±30%).

5.3.4. Discussion

The results gathered by testing the sensor on its own have provided insight into the performance of the sensor. This information was subsequently used as a design input for the conception of the prototypes.

The information gained through these tests can summarized as the following three statements:

- The membrane potentiometer chosen is prone to failure from fluid infiltration if immersed in saline for more than a few hours.
- The maximal resistance varies by approximately 15% between potentiometers.
- The sensor's output does not drift significantly over 21 days for a given measurement.

6. Concept

Three generations of prototypes were produced during this work. The first generation prototype shall be referred to as Prototype 1A with sensors 1A-L and 1A-R designating the left and right side sensors, respectively. The second and third generation prototypes were each produced in 3 identical copies. The same nomenclature shall be applied to each prototype. The second generation prototype shall therefore be referred to as 2A, 2B, and 2C while the third generation shall receive the names 3A, 3B and 3C.

6.1 First Prototype: Proof of Concept

To use the *FlexiPot* sensor in conjunction with the LIVE leads, it is necessary to create a point of contact between the sensor and a fixed reference frame. To achieve this, a bead was fitted on each lead to create a unique point of contact between the sensor and the lead. To ensure a proper reading of the sensor, the bead has to be continually pushed onto the sensor by a guiding part. However, to allow easy movement of the leads in the body, the guide has to apply the right amount of force on the bead so that it doesn't squeeze it and restrict the lead's movement. This guiding part also restricts the movement of the lead to the axis of the sensor and provides a structure for setting a reference frame for the sensor.

6.1.1. Design

This proof of concept prototype was built using conventional tools: drill press, band saw, and grinder. Prior to manually fabricating the prototype, each part's geometry was defined using a modelling software. The result of this modelling can be seen in Figure 17.

Figure 17: Solidworks model of the proof of concept Prototype 1

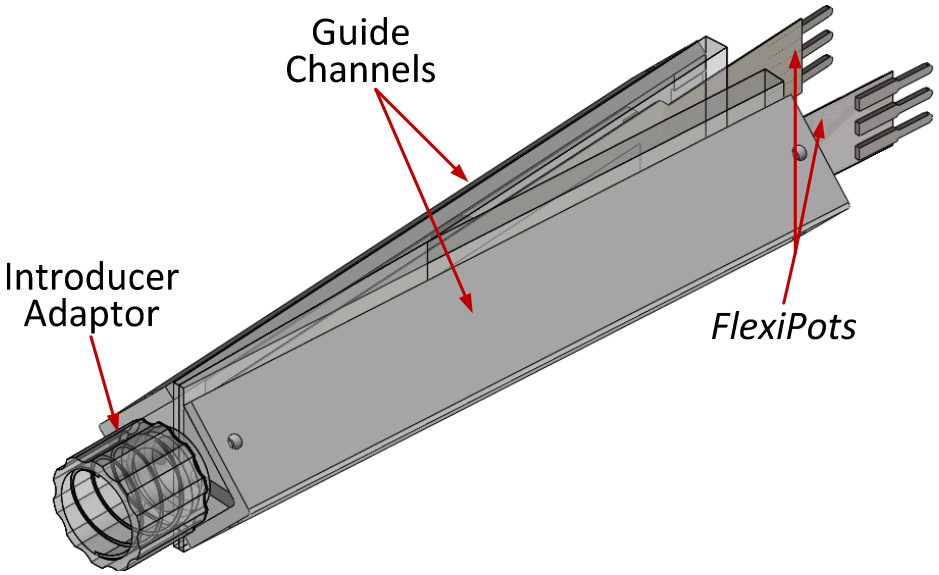

To guide the bead along the length of the sensor, Teflon right angle channels were used in association with ¼" Teflon balls. A hole was bored through each ball using a drill press in order to make them into beads, which could then be fitted onto each lead. In this configuration, the contact between the sensor, the bead, and the channel was minimized to three points of contact. In addition, the choice of Teflon as a material minimized the friction between all components.

The remainder of the housing was made out of sheets of acrylic cut down to size using a band-saw and a grinder for final dimensional adjustments. To allow the leads to converge into the opening of the introducer, each base plate (on which sits each sensor) was grinded at an angle to separate the leads at the smallest angle possible.

To fix the guides to the base plates, triangular support parts were made out of the same acrylic as the base plates. These parts were fitted with a slot for guiding the leads through the unit and the introducer, while maintaining the leads above the active surface of sensor. To allow proper adjustment of the force of the guide onto the sensor (through contact with the bead), the guide were fixed to the triangular supports using small 0-80 screws. The fixation of the triangular supports to the base plate was insured using a silicone-based adhesive. The base plates and sensors were also fixed using the same adhesive.

To reduce the overall size of the prototype, each FlexiPot sensor's tail end was left outside of the housing. To allow the sensors to exit the housing, the triangular support parts distal to the introducer were carved with a slit of the same width as the sensor's tail.

Finally, to give the system its fixed reference frame, the whole unit was made to connect directly to the 12Fr introducer used in pre-clinical trials. To achieve this function, a luer-lock type collar was salvaged from a previously used introducer-dilator system and glued to the end of the housing. Figure 18 shows the proof of concept prototype assembled with the LIVE leads.

Figure 18: Built proof of concept prototype

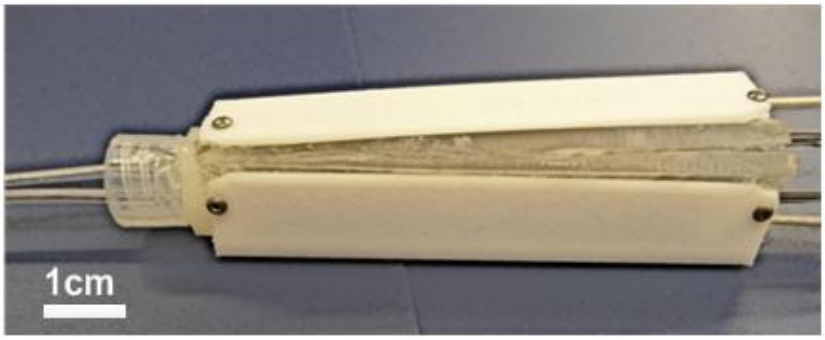

6.1.2. Results

Due to the fabrication method of the proof of concept prototype, only one unit (1A) was built and used during a preclinical experiment. A calibration was performed, but since more descriptive testing ran the risk of damaging the prototype, this work was postponed until after the experiment. Unfortunately, field use had a destructive effect on some parts of the system which made testing all aspects impossible. Amongst the damaged parts were the tail ends of the sensors which were cracked and eventually stopped working. Also some of the holes used to fix the guide were stripped.

6.1.2.1. Lead Travel Test

The leads were pushed through their entire length, but the valid travel was limited by a rise in the force required to move the leads at the ends of the travel. The following table summarizes the results for the two sides tested for the same prototype. The travel reported was limited by the force required to move the leads at both ends of the sensor active length.

Therefore, the force reported represents the travel within which the contact with the sensor was good, and the force required to move the leads was constant.

Table 5: Travel results summary for Prototype 1A

	Linear Travel	Angular Travel
1A-L	5.3mm	360 degrees
1A-R	4.6mm	360 degrees

6.1.2.2. Movement Resistance Test

Overall performance during the preclinical experiment was noted as satisfactory. Compared to the usual resistance to movement offered by the vasculature, the added resistance of the depth sensor was not noted as significant by the user.

However, bench testing showed different results. The following table summarizes the results of the movement resistance test.

Table 7: Movement resistance test results for Prototype 1A

	Push Force (N)	Pull Force (N)
1A-L	4.47 ±0.21	4.32 ±0.34
1A-R	0.90 ±0.10	1.02 ± 0.21

6.1.2.3. Accuracy/Repeatability Test and Pre-Clinical Validation

The prototype was used to perform nerve mapping in a preclinical experiment. To verify the sensor's output in vivo, every time an electrode was moved, the electrode's position was measured using a ruler as well as with the sensor. The values obtained were then compared and can be seen in Figure 19. The results illustrated only represent single measurements for each depth, done in vivo.

Figure 19: Comparison of Prototype 1A measurements vs. ruler measurements made during a pre-clinical experiment

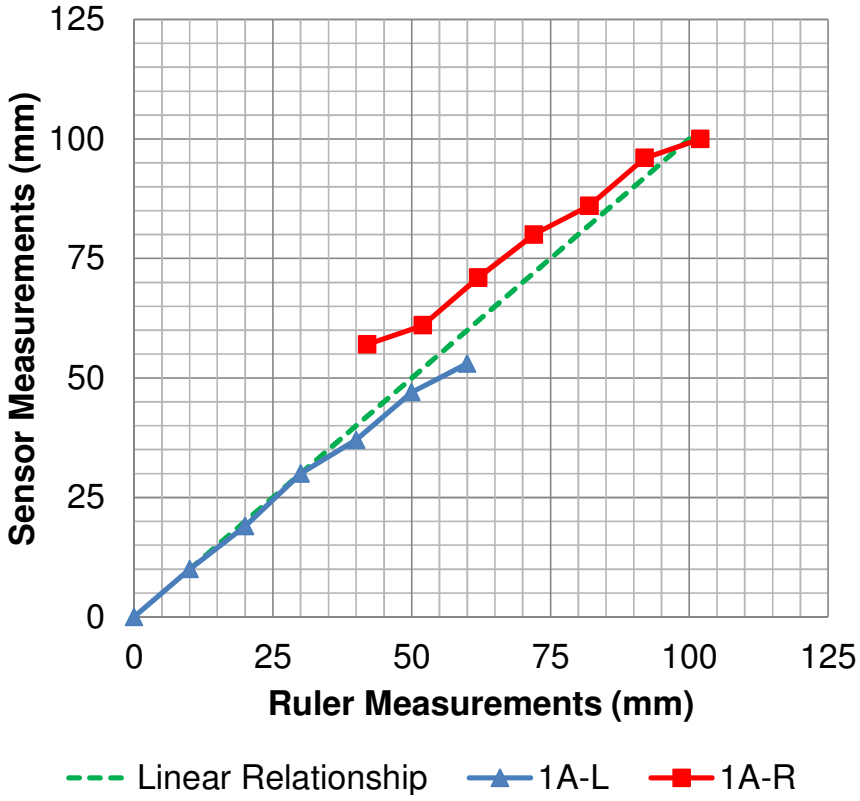

The difference between the ruler measurements and left sensor can be seen as ranging from 0 to 7mm. This difference is significantly larger for the right sensor, as it goes from 2 to 15mm. The discrepancies are mainly associated with two issues: the first was an unwanted movement between the Teflon ball and the electrode, and the second was a bad contact between the bead and sensor. Both problems are explained in detail in the following section.

Since part of the difference reported in the preclinical results had been identified and could be avoided, corrective measures were taken when performing the accuracy and repeatability test. However, only one side of the prototype was tested using this method since the second side was no longer functional at the time of the test.

Table 6: Accuracy/repeatability force results for 1st prototype

	Average Accuracy (mm)	Repeatability (mm)	Maximum Error (mm)
1A-L	1.26	1.18	3.28
1A-R	N/A	N/A	N/A

The following graph shows the average error for each position at which the sensor was tested. The error bars shown on the graph represent the standard deviation of the error for each of the 5 positions which were tested.

Figure 20: Accuracy/repeatability results shown as the difference between each measurement and the true value (Prototype 1A-L)

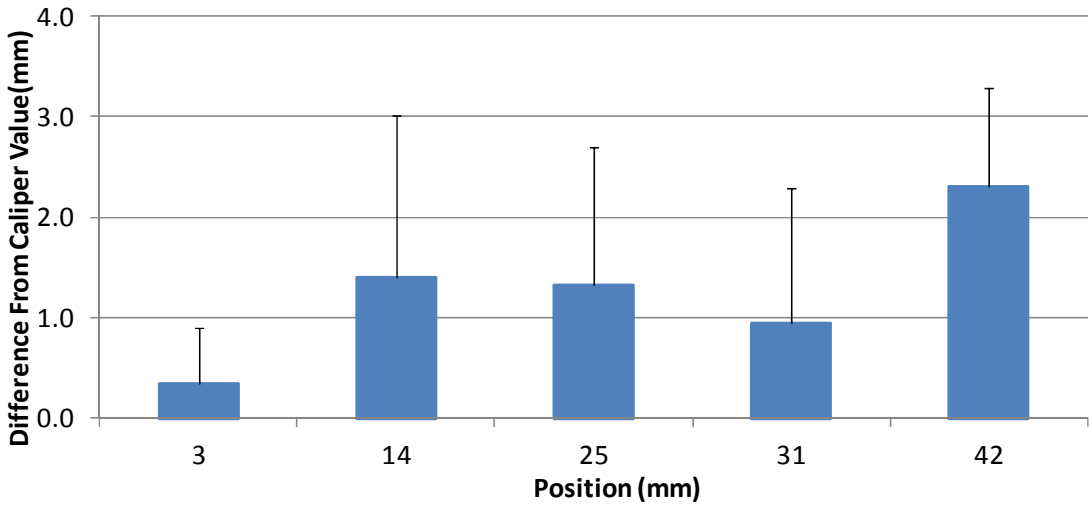

6.1.2.4. Fatigue Test

Since Prototype 1A did not meet the force criteria of the push/pull requirement, or the accuracy/repeatability requirements, the fatigue test was not performed. In fact, the overall performance of the prototype suggests that the cycling performed through calibration and the previous tests were enough to deteriorate the performance of Prototype 1A.

6.1.3. Data Analysis

6.1.3.1. Movement Resistance Test and Travel Test

The force required to move the leads inside their respective tracks showed a significant difference between the two sides of Prototype 1A. Additionally, the results were far from the desired level of less than 0.75N, which was previously established as a safety margin. This variability could be attributed to uneven fabrication of the triangular support. Small variations in the dimensions of these parts could greatly vary the force with which the guides pushed down on the bead and this would have a direct impact on the force required to push or pull the leads.

The same problem also seemed to be at the origin of the limited travel of the leads within each side of the housing. By fixing the guide at punctual locations along their length, the guides became deformed where the screws were, thus restricting the movement of the bead and the lead.

6.1.3.2. Accuracy/Repeatability Test and Pre-Clinical Validation

Most of the difference in measurement values between the ruler and sensors can be traced back to the construction of the leads themselves. The shaft on which the electrodes were fixed could be moved independently from the freely floating, unadhered polymer sheath onto which the Teflon bead was fixed. When the shaft moved independently of the sheath, the sensor did not register any change in position. As can be seen in the following set of pictures, wrinkling and stretching of the outer sheath allowed the electrodes to travel independently from the bead over more than 15mm, thus creating a variable offset between the position registered by the sensor and the actual position of the electrode array.

Figure 21: Relative movement of the Prototype 1 lead shaft inside its polymer sheath (a) in its normal position and (b) as the sheath wrinkled and allowed movement of the shaft independent from the bead

(a)

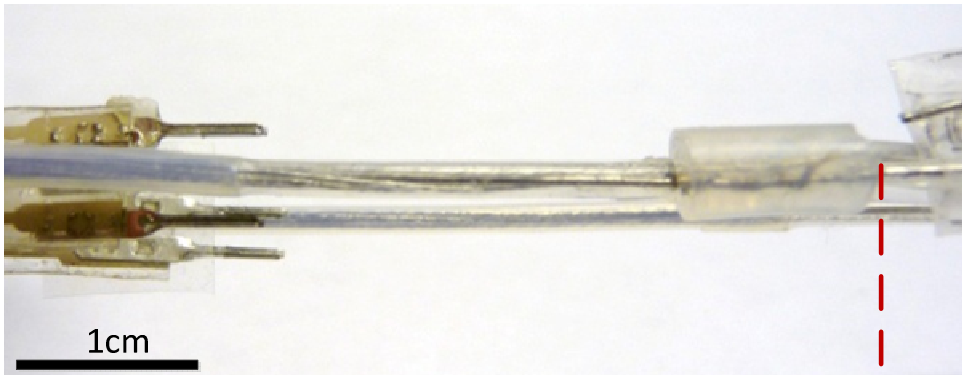

(b)

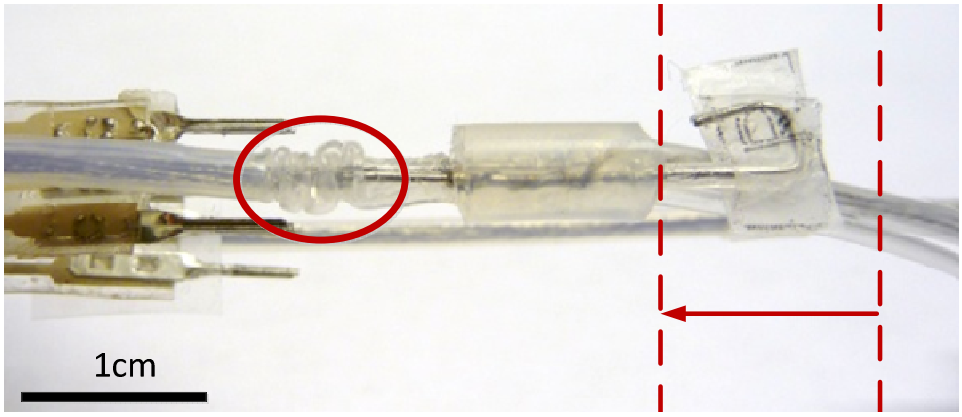

Knowing this information about the deformability of the lead insulation, it was possible to eliminate most of this error from subsequent tests. To accomplish this, the caliper was attached to the portion of the lead distal to the silicone sheath (left of the circle in Figure 21b). However, this change was not sufficient to yield results out of Prototype 1A which satisfied the requirements. Although the sensor offered a smooth output, an average error of more than 1mm was measured. The error is thought to have originated from a poor fixation of the Teflon bead to the outside of the lead. This fixation might be prone to some compliance which may result in an error of 1 to 2mm.

Neither the accuracy nor repeatability requirements were fulfilled with Prototype 1.

6.1.4. Discussion

With the triangular support parts, shown in Figure 22, requiring dimensions ranging from approximately 2 to 8mm with a margin of error of about 0.5mm, the making of such parts involved laborious trial and error. This iterative process and the poor results it generated confirmed that the manufacturing of the system would require a more controlled process for further preclinical testing.

Figure 22: (a) Solidworks model of the triangular support parts for the proof of concept and (b) a picture of assembled part

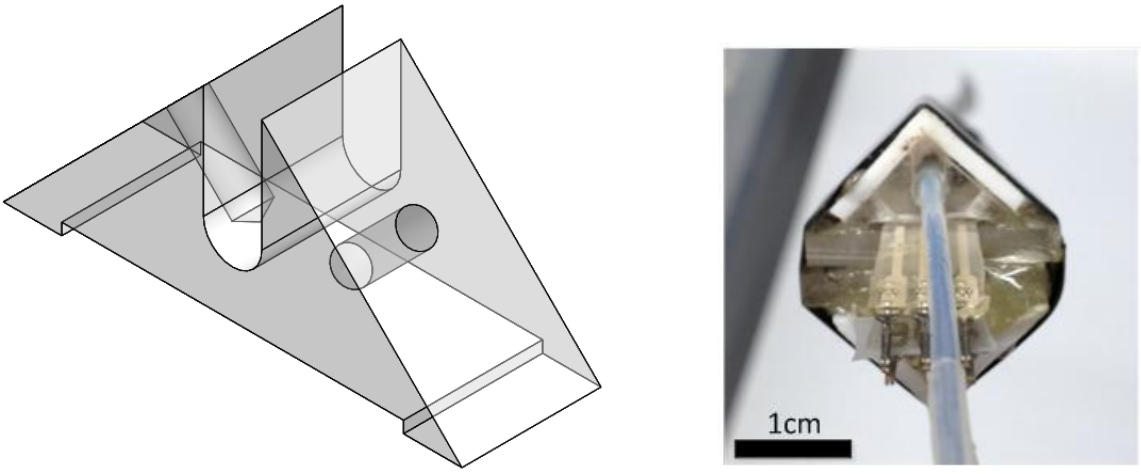

(a) **(b)**

From the analysis of the results, we found that problems in Prototype 1 originated from using 0-80 screws self-threaded through acrylic for fixing the guide into place. After multiple tightening and removing of the screws, the holes quickly lost their thread and proper fixation

became difficult, if not impossible. Adjustment of the pressure of the bead using the screws was also dysfunctional mostly because of the limited stiffness of the right-angle guides and the punctual application of pressure by the screws. As a result, the bead would not always remain in contact along the whole length of the sensor. In other words, it would become too tightly squeezed when in proximity to a set of screws, and too loose in other positions. When the bead was not in contact with the sensor, the electrical tension sensed by the system was therefore influenced by other signals acquired at the time.

Another element that required improvement in later prototypes was the fixation of the Teflon bead onto the outer sheath of the lead. Considering that Teflon was chosen for its low coefficient of friction, this also comes with the disadvantage of being difficult to fix in place. Many attempts were necessary to glue the beads in place using a Teflon etching solution and silicone adhesive. Despite all efforts, the fixation remained precarious throughout the life of Prototype 1A, resulting in shifting of position as previously described. Therefore, a different fixation method or bead material should be considered for subsequent designs.

The use of a luer-lock type sleeve at the end of the housing also made it impossible to dissociate the P-Mode unit from leads. Even though the guides were removable because of their method of attachment, the luer-lock sleeve had to be glued to the proximal side of the unit, therefore constraining the leads.

Lastly, leaving the tail end of the sensors unsupported by the housing caused the sensors to sustain damage and eventually stop working adequately. By being unsupported and free to move, this section of the sensors became susceptible to the flexion and torsion caused by tension in the cable linking it to the data acquisition system. By using Prototype 1A on multiple occasions (for testing and various demonstrations), the sensors eventually cracked and ceased to produce reliable signals.

Figure 23: Example of the damage inflicted on the tail end of the sensors by the connectors in Prototype 1A

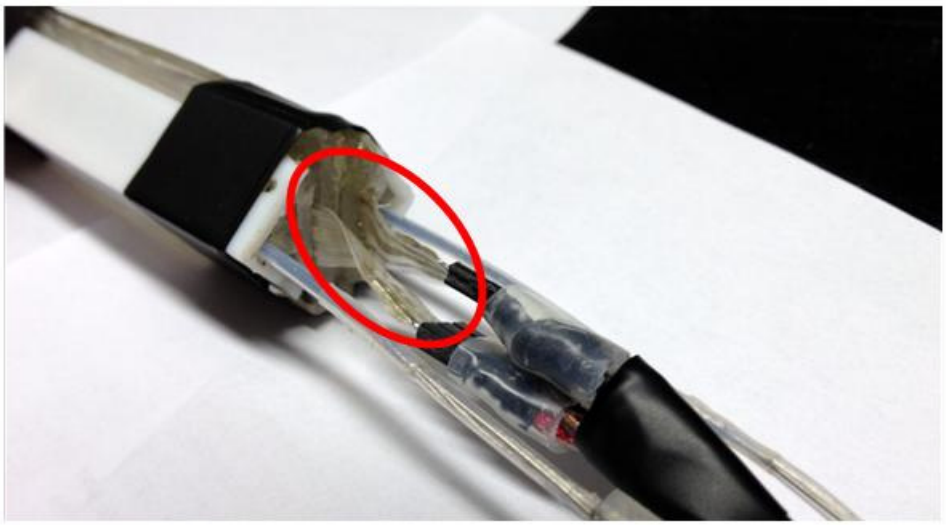

Despite the limitations of this first prototype, the proof of concept was successful at showing that this concept could be compact. Each of the problems highlighted here can be corrected by improvement in the design.

6.2 Second Prototype

With the “membrane potentiometer and bead” concept validated by the proof of concept, a second prototype was produced using a rapid prototyping method. The *PolyJet* printing process from the manufacturer *QuickParts* was chosen as described in the next section. By using this manufacturing process, the fabrication capabilities were improved significantly. According to the company’s website, the resolution of their process is 16 µm, and allows for features as small as 635 µm. Solving problems highlighted by the proof of concept, such as the variable contact of the ball on the sensor, and building an assembly which was easily removable from the leads, was made possible by the change of manufacturing process.

6.2.1. Design

While conserving the overall idea behind the proof of concept, the second design exploited the greater precision offered by 3d printing for nearly all of its features. The fixation method to the introducer, the housing of the *FlexiPot*, the fixation of the guides, and the

assembly of the sensing unit to the leads were all changed significantly. Figure 24 shows the prototype's CAD model.

Figure 24: Solidworks model of Prototype 2

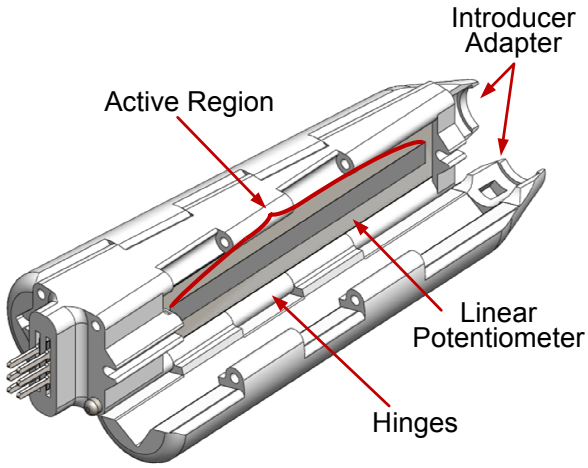

To allow the sensing unit to be detached and fixed onto the LIVE leads, hinges were added to the guides of this prototype. The hinges were made as part of the guide and base parts and required only the addition of a 1/16" metal pin to articulate each hinge. With each guide part hinged on either side, it could potentially be articulated from either side. However, only one of the metal pins was made to be easily removable, so that one side is used to open the housing while the other one always remained closed. By using pins to close the guide running alongside the sensors, the height of the guides relative to the base part was held constant andhelped to provide a more uniform contact pressure.

To help with the uniformity of the contact between the Teflon ball and the sensor, the base part and guide were designed to allow for adjustment of the pressure made on the bead. To do this, the distance between the FlexiPot (on the base part) and the guide was purposely made larger than the size of the Teflon ball. The potentiometer was then mounted on a thin compliant polymer layer thicker than the said "extra space". By doing so, the contact between the guide, bead, and sensor was made continuous throughout the whole length of the sensor while allowing for a controllable contact force proportional to the compliance of the material used to mount the sensor. Figure 25 illustrates this concept. To compensate for the extra space left for the polymer layer, a smaller bead was used (3/16" instead of 1/4").

Figure 25: Illustration of the strategy used to maintain a light continuous contact between the sensor and Teflon bead in Prototype 2

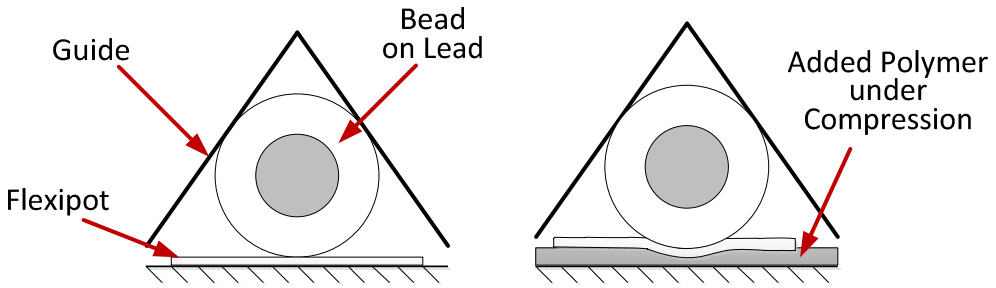

Making use of the hinged parts and the greater precision of 3D printing[8], the luer lock of the previous prototype was replaced by a "snap-on" collar split into two halves associated with each hinged guide. Shaped to fit the hub of the introducer used by the Neurokinesiology lab, each hinged guides was fitted with one half of a collar as shown in Figure 26a. With the hinged guides closed, these half cylinders form a collar with a lip made to clip onto the large thread of the luer-lock hub. As shown in Figure 26b, the introducer hub was also made out of two halves separated by a gap of about 1mm. Therefore the two sides of the connection offered enough compliance to mate and unmate without much effort, while maintaining a reliable connection.

Figure 26: (a) Hinged collar concept and (b) the hub of the introducer

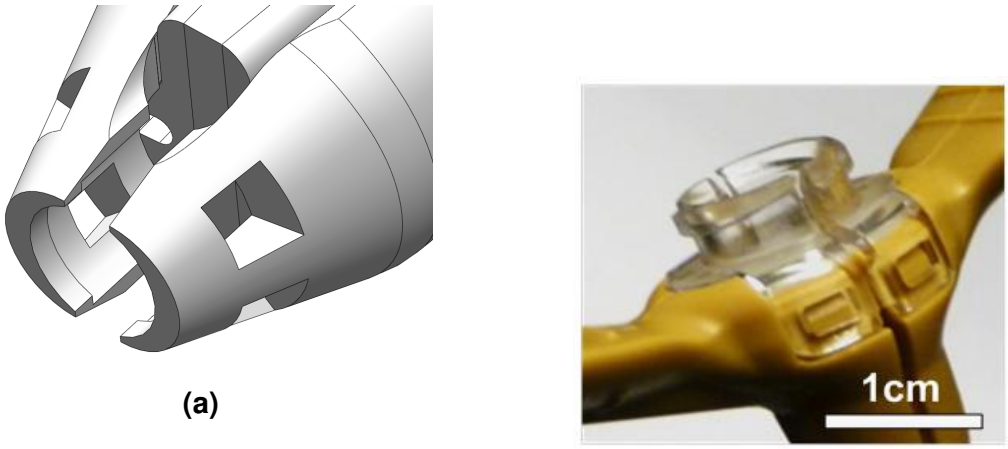

(a)

[8] More information on the 3D printing process and material are available in Appendix C.

(b)

To fix the problem of durability of the FlexiPot sensors' tail end, the entire length of each sensor was included in the housing of the unit. The base part was designed to include a thin curved tunnel to cover the sensor's tail end. At the same time, this tunnel was designed to bring the tail ends close to the center plane of the base part. By doing so, the pins of both sensors were grouped, allowing for the use of one connector for both sensors. This feature also allowed greater clearance at the back of the housing – where each lead entered the unit – while slightly reducing the length of the prototype. Figure 27 provides more detail on this feature.

Figure 27: Sectional view showing the tunneling feature of Prototype 2

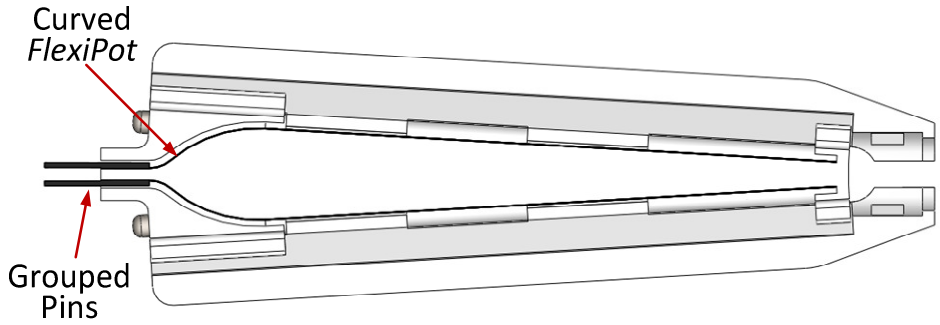

Considering that the design required dimensions as small as 0.75mm, a process with high resolution had to be chosen to fabricate the prototype. However, the need for high resolution was also balanced with a need to limit the cost of each part. A third important element in choosing the manufacturing process was the surface finish, in order to have a smooth movement of the lead through the housing. The process filling all three criteria was a UV curing photopolymer printing process called *PolyJet*. More information is available in Appendix C about the different 3D printing processes considered.

Considering the shortcomings of Prototype 1 attributable to the integration with the LIVE leads, necessary steps were taken to avoid the problems previously experienced.

6.2.2. Results

The change to *PolyJet* 3D printing produced accurate results and a smooth surface finish. The parts received corresponded to the high expectation held towards the process. All

important dimensions were respected and the material displayed good resilience although the parts remained brittle. The prototype can be seen in Figure 28. The surface finish also allowed a good sliding contact between the Teflon bead and the guide part.

Figure 28: 3D printed Prototype 2 seen opened and without LIVE leads.

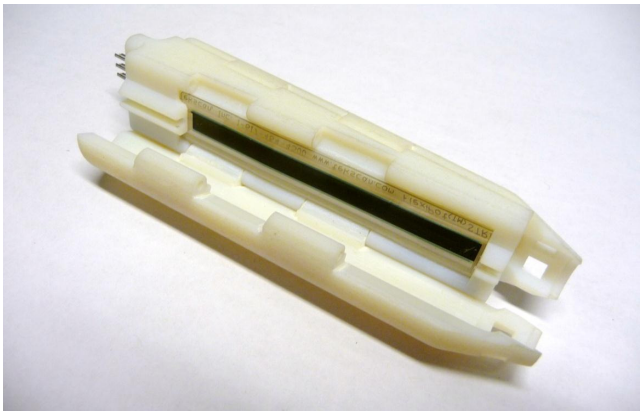

Like any prototype, parts designed to have a tight fit are always susceptible to being slightly too loose or too tight. However, in this case all fits worked as intended. The hinged collar designed to mate with a Greatbatch 12 French introducer allowed very little post-production adjustment but still produced the intended result. The unit could therefore be clipped onto the introducer and removed without much force required. Figure 29 shows the P-Mode sensor and introducer assembled as it would be during normal operation.

Figure 29: Prototype 2 assembled with a Greatbatch 12Fr introducer

Prototype 2 could not be tested in vivo, because no animal experiments were performed between May 2011 and the completion of this thesis. However, Prototype 2 was submitted to the same series of bench tests described previously. All three units produced were tested

according to the Travel Test, and Movement Resistance Test and Accuracy/Repeatability test, while unit 2A was also tested according to the Fatigue Test.

6.2.2.1. Travel Test

The leads were successfully pushed through the entire length of the prototype. The leads could also be rotated entirely. However, the left side track failed to deliver a proper signal past 57mm as it appeared the bead was reaching the end of the sensor. The following table summarizes the results for the two sides tested for the same prototype.

Table 7: Travel test results summary for Prototype 2

	Linear Travel	Angular Travel
2A-L	57.1mm	360 degrees
2A-R	60.0mm	360 degrees
2B-L	60.0mm	360 degrees
2B-R	60.0mm	360 degrees
2C-L	60.0mm	360 degrees
2C-R	60.0mm	360 degrees

6.2.2.2. Movement Resistance Test

The force required to move the leads through the housing was recorded using the method previously described. The following table summarizes the results of this test.

Table 8: Movement resistance results summary for Prototype 2

	Push Force (N)	Pull Force (N)
2A-L	0.15 ±0.04	0.18 ±0.04
2A-R	0.15 ±0.05	0.12 ±0.04
2B-L	0.16 ±0.05	0.13 ±0.05
2B-R	0.14 ±0.02	0.15 ±0.06
2C-L	0.17 ±0.03	0.16 ±0.04
2C-R	0.16 ±0.05	0.13 ±0.06

6.2.2.3. Accuracy/Repeatability Test

Values for accuracy and repeatability were obtained by performing the protocol described in section 4.2.2. Table 9 summarizes the results of this test for the three prototypes tested.

Table 9: Accuracy/repeatability results summary for Prototype 2A

	Average Accuracy (mm)	Repeatability (mm)	Maximum Error (mm)
2A-L	0.09	0.04	0.32
2A-R	0.19	0.03	0.32
2B-L	0.15	0.05	0.23
2B-R	0.12	0.03	0.31
2C-L	0.14	0.04	0.26
2C-R	0.19	0.04	0.30

The results of the test can also be visualized in more detail as the average error of each individual trial as compared with the calibrated value. The error bars represent the standard deviation of each position.

Figure 30: Accuracy/repeatability results shown as a difference between each measurement and the caliper measurements for Prototype 2

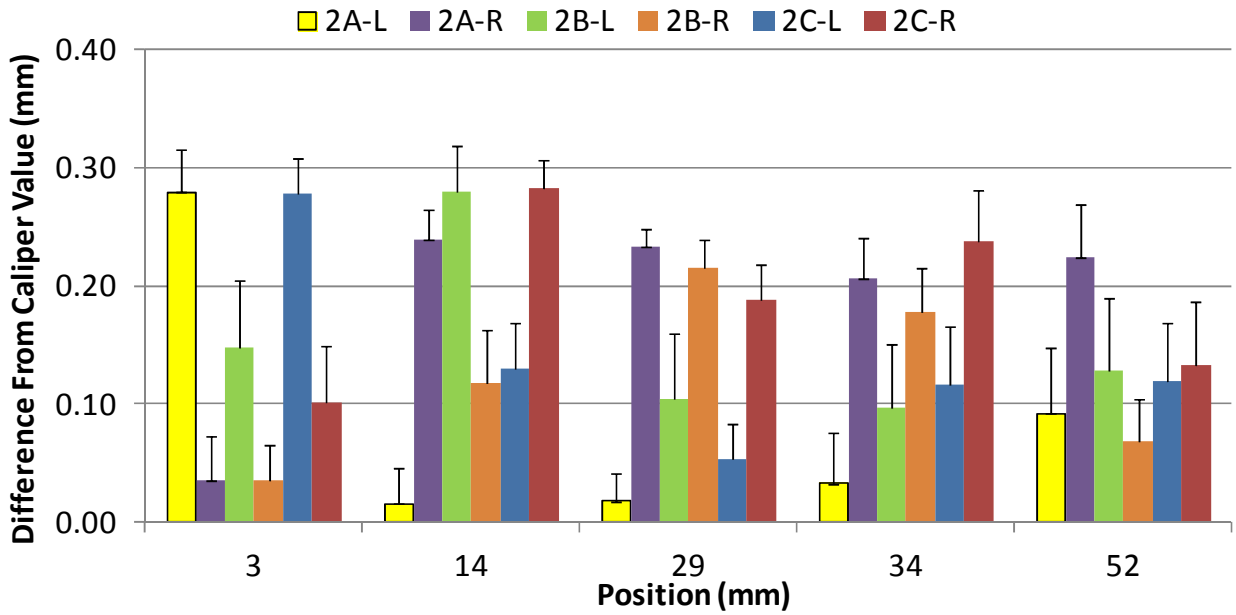

6.2.2.4. Fatigue Test

Values for push/pull force, accuracy and repeatability were obtained after 50 cycles of movement through the full range of the sensors. Table 10 summarizes the results of the accuracy test and the movement resistance test after the cycling occurred.

Table 10: Push/pull and accuracy/repeatability results summary for fatigue test of Prototype 2A

	Avg. Accuracy (mm)	Repeatability (mm)	Max Error (mm)	Push Force (N)	Pull Force (N)
2A-L	0.06	0.06	0.29	0.14 ±0.05	0.13 ±0.06
2A-R	0.14	0.03	0.27	0.15 ±0.04	0.10 ±0.04

A student t-test done between each value before and after the fatigue test revealed no significant difference between both results groups. The result of the t-tests can be consulted in Table 18 in Appendix E.

6.2.3. Data Analysis

6.2.3.1. Travel Test

The travel of both sides of the prototype was higher than the required 50mm set in the requirements. However, for Prototype 2A, one of the tracks failed to reach the full 60mm that it was designed for. The reason for this shortcoming was thought to lie in the positioning of the membrane potentiometer. It is possible that the sensor shifted by a few millimetres before it finished being glued in place.

Full angular rotation was also achieved for both sides of the prototype. However, this movement was noted as jerky or hard to control. This can be attributed to an eccentricity in the Teflon beads used.

Apart from this minor issue, Prototype 2 was shown to fulfill both the linear and angular travel requirements.

6.2.3.2. Movement Resistance Test

Minimal force was required to move the leads. The results showed a much smaller standard deviation than Prototype 1, suggesting greater repeatability between the two sides of Prototype 2. This repeatability can be attributed to the manufacturing process chosen because of its much greater accuracy. The use of a compliant backing layer for the potentiometer is thought to have also contributed to this result.

The forces required on all sides of Prototype 2 were lower than the level specified in the requirements, with an average force of 0.15N.

6.2.3.3. Accuracy/Repeatability Test

The accuracy results reported for prototype 2 were within the required ±1mm accuracy. The average error was, at worst, 0.19mm from the caliper value, while the worst individual error seen during the test, 0.32mm, was also under the 1mm accuracy threshold. The repeatability of both sides was also under the maximal variability of the requirement. The results were on average 0.14mm away from the caliper value with a distribution of results that spanned ±0.04mm.

Both precision and accuracy results were better than the values suggested by the manufacturer of the linear potentiometers. In fact, the manufacturer only states that repeatability and linearity error are below 1 and 2% of full scale, which appears to be a conservative estimation according to the results of this test. The results found in this test suggest a repeatability of 0.1% of full scale.

6.2.3.4. Fatigue Test

After performing 50 cycles for both sides of the prototype, the results of force and position remained satisfactory. Not only did they remain under their maximum value established in the requirements, but no significant difference was seen between the original tests and the repeated tests done after the fatigue cycling.

The fatigue test showed that the prototype maintained its performance level beyond its expected normal use.

6.2.4. Discussion

Despite great progress from the proof of concept, a need for few potential improvements was noted.

By using smaller Teflon balls (from 1/4” to 3/16” in diameter), the eccentricity of the bore drilled using a press drill was more perceptible. Without any specific setup to align the drill bit with the center of the ball, the beads produced had a bore that was slightly off from the center axis of the ball. The main consequence of this eccentricity was a reduced fluidity in adjustments of the angular orientation of the lead. This problem could easily be solved by either using a jig that would center the ball with the drill bit, or by simply buying off the shelf Teflon beads.

However, off the shelf Teflon beads have yet to be found, and therefore a change in material could potentially be adequate.

Figure 31: Environmental noise measured by Prototype 2.

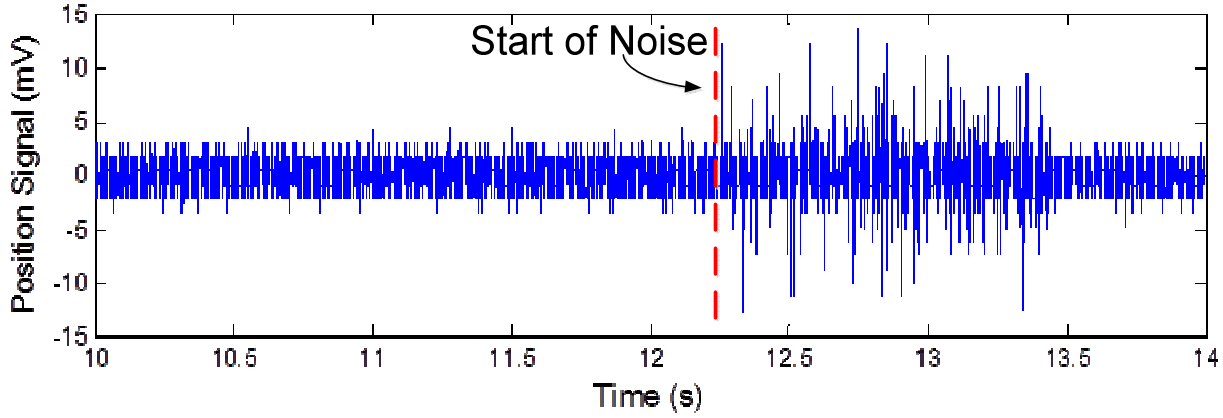

Because the contact between the ball and sensor was able to be maintained at all times and the force required to move the lead was minimal, it was possible to observe a low amount of noise on the raw signal. This noise could be quantified as approximately 5mV peak to peak at most. With a calibration of about 14mm/V, the noise level was not large enough to affect accuracy or repeatability. However, in a situation where multiple other medical devices surround the positioning system, this noise amplitude could potentially increase enough to induce an oscillation in the signal shown to the therapist.

6.3 Third Prototype

With the progress of Prototype 2, few improvements were needed to make the system's performance to a satisfactory level. However, multiple changes were made in order to bring this concept one step closer to being eligible for approval by the appropriate regulatory bodies.

6.3.1. Design

The first important change in Prototype 3 was to adapt it to a new LIVE lead design. The membrane potentiometer concept was adapted to a multilumen catheter, instead of an introducer. At the same time, a few functional improvements were made, including protecting the potentiometer's pins from contact with fluids, adding noise protection to the system and

facilitating a smoother rotation of the leads. Figure 32 shows a model of Prototype 3 (bottom half only).

Figure 32: Prototype 3 annotated model

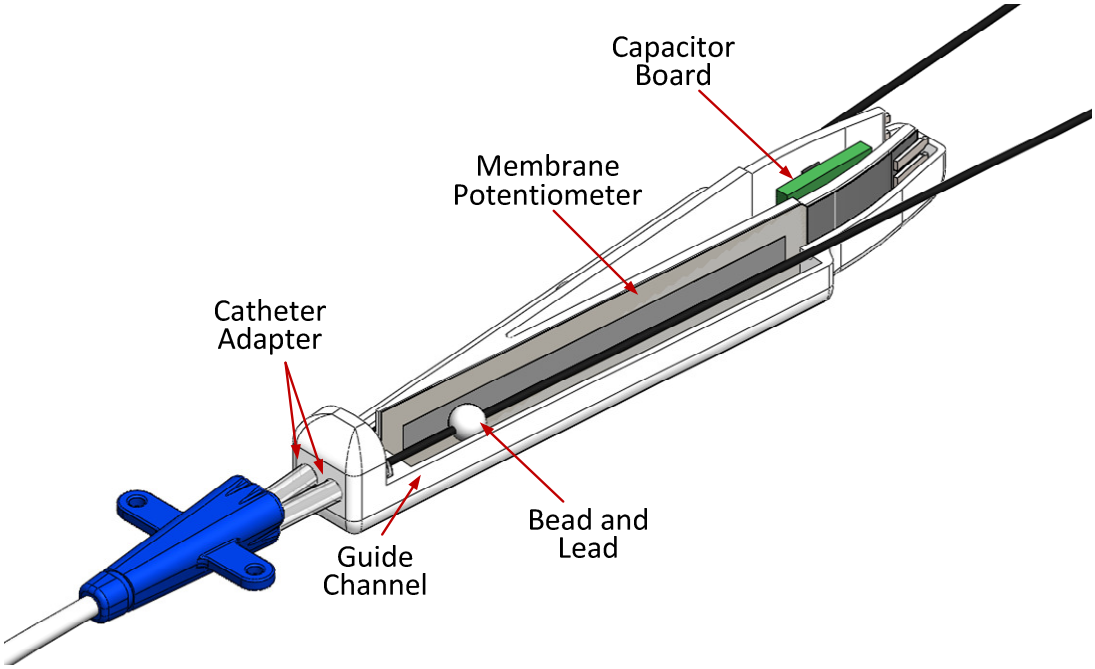

Note: Wires between the capacitor board and the sensor contacts are not represented in this model.

The new lead design used a commercially available 5 lumen 8.5Fr central line catheter manufactured by Teleflex (Figure 33). The lumens were externally accessible through 5 polyurethane extension tubes disposed on two rows on the catheter's hub. The tubes of the largest two lumens, which were disposed side by side, were used to introduce each of the intravascular leads. By inserting the leads directly through the lumens of an intravascular catheter, the housing of the position sensing unit could be referenced directly to the catheter hub. The tubes were cut to a 1cm length and glued directly into the housing of the sensor. To do this, the housing included two bores to accommodate the tubes, which were aligned with the membrane potentiometers.

Figure 33: 5 Lumen, 8.5Fr Arrow central line catheter (Teleflex).

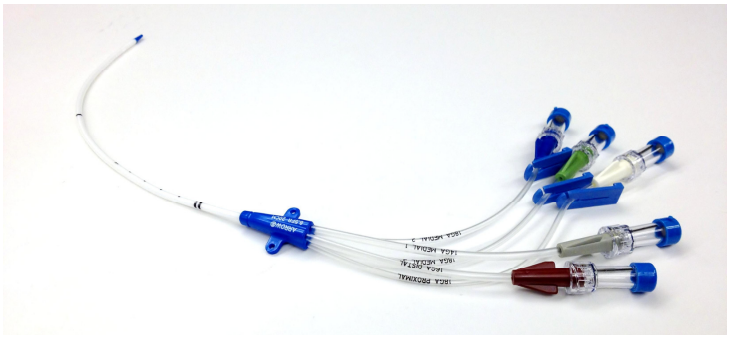

With the tubes having direct access to the vein, it was necessary to install valves to limit the backflow of blood into the positioning system's housing. To do this, a silicone sheet of 2mm in thickness was punched into a circle and glued to where the tubes met the housing. A small hole was punched using a hypodermic needle smaller than the size of the leads (Ø1.30mm). The leads would then fill the hole and stretch it enough to provide a barrier blocking fluids from getting into the unit. The dimension of the hole made into the membrane had to be large enough to not induce too much frictional resistance, but still maintain a good seal. Additionally, to improve the sensor resistance to fluids that may break through the valve, the sensor contacts were encapsulated in epoxy.

Figure 34: Valves without the top part assembly

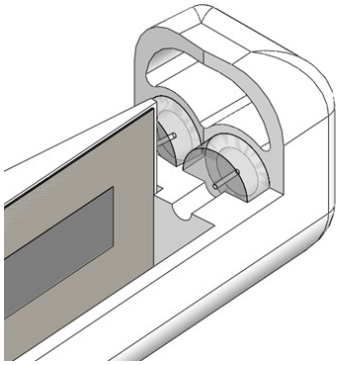

Because of the results of Prototype 2 which showed a susceptibility to environmental noise as shown in Figure 31, a method to smooth the signal was implemented on Prototype 3. The power supply wire was rerouted to the center of the housing where it passed through a capacitor. Bypass capacitors act mostly like low pass filters by smoothing the AC component of

the power supply. The capacitor chosen for the circuit was a 100nF based on standard practice for this kind of circuit[9].

Figure 35: Bypass capacitor circuit diagram

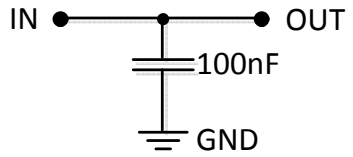

Once filtered, the signals were extracted through a connector mounted to the housing. Although this connector was not hermetic because of cost and size constraints, it was positioned where it was not as likely to be exposed to fluids, unlike the previous prototypes.

At the heart of the sensing unit, the concept of the membrane potentiometer and the bead remained mostly untouched apart from slight refinements. To improve the fluidity of the lead's rotational movement, a simple jig was made in order to bore each Teflon ball. A hole of the same diameter as the ball was drilled halfway through a ¼" plexiglas strip. A smaller hole was then drilled through the strip concentric with the larger hole. This smaller hole was then guided by the converging shape of the larger bore. A ball was put inside of the larger hole and clamped upside down on the drill press table, where alignment of the drill bit guaranteed that the hole was centered along the central axis of the ball.

Figure 36: Ball drilling setup

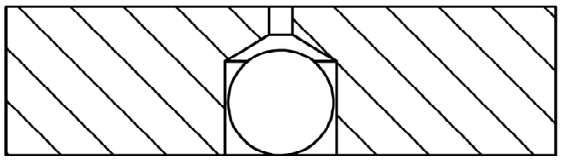

The hinge system was also eliminated and replaced by a simple screw fixation using one 2-28 screw placed in the middle of the housing. To facilitate assembly, the top part was

[9] Information from Introduction to Circuit Analysis and Design by Tildon H. Glisson, p266.

designed with a bored protrusion for screw alignment. To constrain the movement of the two parts and to further reduce possible fluid penetration into the housing, the protrusion used to fix the screw also prevented rotations of the top part by assembling with a female end of the same geometry.

Figure 37: Housing screw and protrusion on bottom part (left) and top part (right)

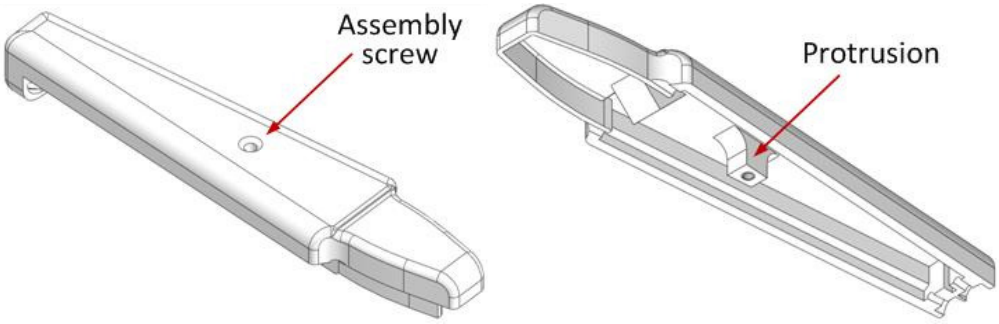

The bottom part also included flat surfaces on which each of the potentiometers rested, as well as half of the bead's guide. The other half of the guide was designed as part of the top half that closed the assembly. The guides were also positioned at an angle like the previous prototypes. This angle was set to ease lead transition from the hub to the catheter shaft. To do so, the angle was chosen to approximate the angle at which the leads were spread when coming out of the hub (see Figure 38). With the leads offering very little resistance when spread at angles of 5 to 10degrees, the angle between the leads was set to 8 degrees.

Figure 38: Angle of separation between leads as they come out of the Arrow catheter hub

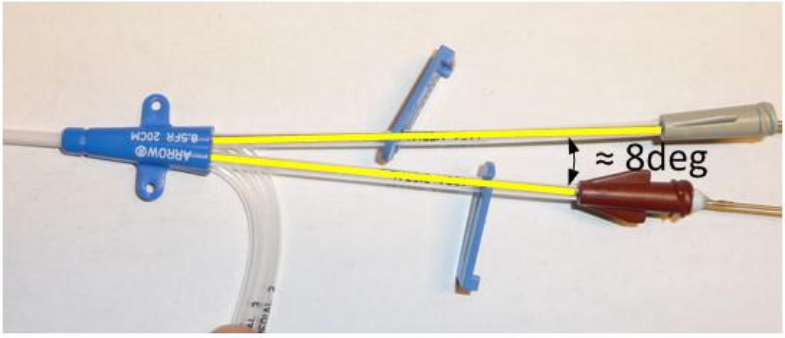

Given the good results of Prototype 2 and continuity in the required resolution of the process, the same 3D printing manufacturing process and material as for Prototype 2 were used for manufacturing Prototype 3.

6.3.2. Results

Few results were extracted from Prototype 3 because of the poor quality of product received from the manufacturer. Unlike the first iteration of 3D printing, Prototype 3 had a rough surface finish that did not allow proper movement of the leads and the surfaces on which the beads were meant to slide were made in a step-wise fashion. For this reason, the beads were not able to move through the guides. The parts were therefore sent back to the manufacturer for reimbursement. As a result, none of the tests previously described were performed using Prototype 3. Each of the requirements associated with those tests cannot therefore be considered as met by Prototype 3.

Figure 39: Surface finish of Prototype 3

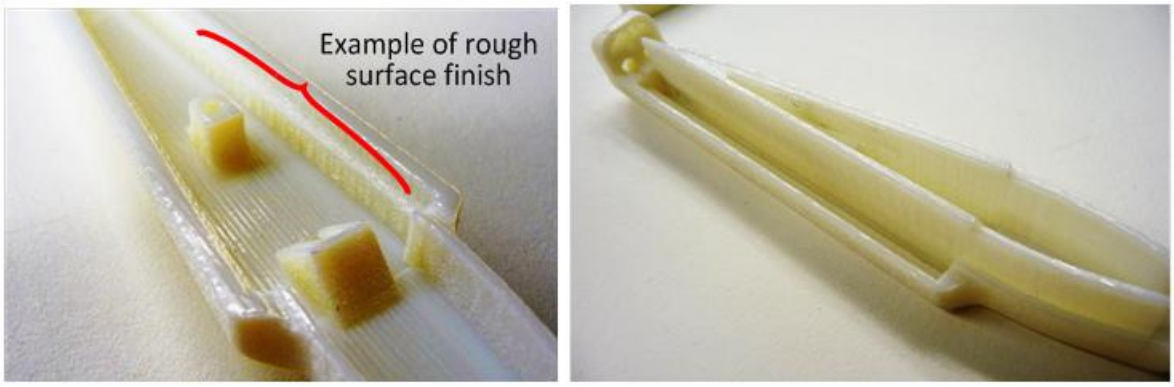

6.3.2.1. Noise Protection Test

Nevertheless, the concept suggested for reducing susceptibility to noise was tested. By generating electrical noise using a wall powered drill, the system's sensitivity to noise was tested. In a normal situation, this noise might emanate from other devices using electric motors, pumps, or systems with electromagnetic properties. Circuit diagrams for the bypass used and the positions in which it was tested are showed in Figure 35 and Figure 40. Figure 42 shows the results of 3 different noise cancellation strategies compared with two baselines (with and without noise).

Figure 40: Diagram of the three positions where the capacitor bypass was tested

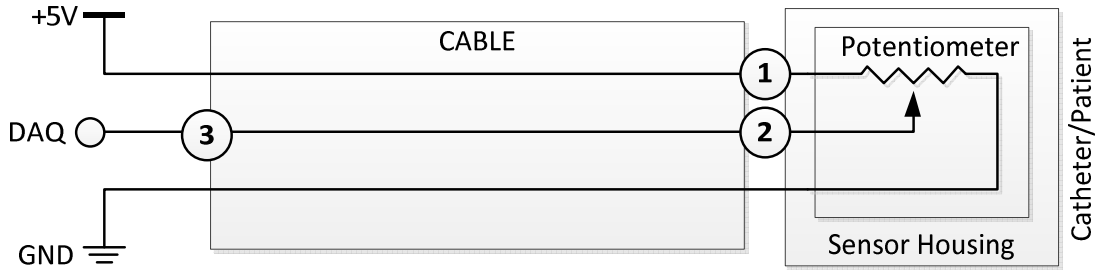

Applying a capacitor bypass to the power supply at its entry point to the system's housing did not reduce the amount of noise. The noise amplitude using this strategy, 24mV, was actually higher than the baseline noise amplitude of 21mV. The same strategy was used to bypass the position signal, also within the system's plastic housing. The amplitude of the signal was reduced to 17mV. Lastly, using the capacitor bypass at the end of the cable, before it entered the data acquisition system (DAQ), produced a peak-to-peak noise amplitude of 1.6mV.

The use of a capacitor bypass did not affect the calibration of the sensor. All measurements taken across the length of the sensor, with and without the noise cancelation, showed results consistent with the repeatability shown in section 6.2.2.3. The average difference between corresponding measurements is the same as the repeatability of 0.04mm reported for Prototype 2.

Figure 41: Difference in signal amplitudes with and without a capacitor bypass

	Position measurements (mm)						
Position Signal (V)	**0**	**10**	**20**	**30**	**40**	**50**	**60**
With Bypass	0.656	1.368	2.108	2.812	3.505	4.224	4.921
Without Bypass	0.640	1.365	2.103	2.811	3.509	4.223	4.921
Difference (mm)	0.22	0.04	0.07	0.01	-0.06	0.01	0.00

Figure 42: Noise cancelation results

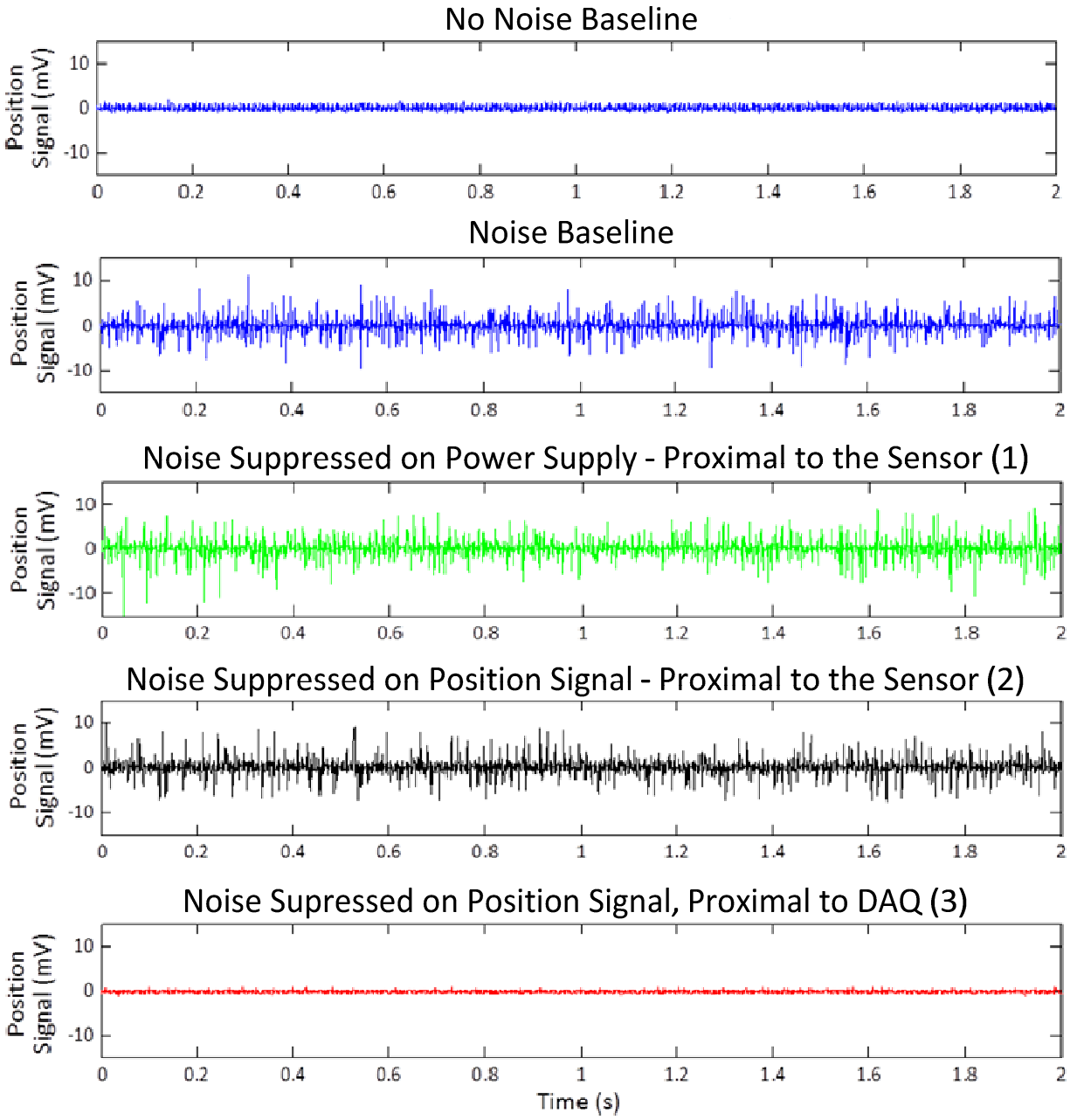

Note: Four different noise cancelation configurations using a capacitor bypass on the power supply or position signal. The signals shown represent the behaviour of the system when exposed to large amounts of noise compared to a baseline with no noise.

6.3.2.2 Valve Test

Hermeticity tests were performed to qualify the performance of the valve concept. To do this, three valves with different dimensions were tested. The valves were identical except the through

hole size used to pass the leads. The hole was made with tools of three different diameters (∅ 0.80mm, ∅ 1.30mm, and ∅1.68mm) and all tested for the same lead dimension (∅1.30mm). To test each configuration, each valve was fixed to the end of a syringe. The syringe was filled with water and used to simulate blood pressure.

Two tests were conducted. The first test used a 1.34kg weight placed on the syringe handle to simulate blood pressure. With a syringe diameter of 25mm, the pressure resulting from this force was equal to 200mm of mercury, a conventional high blood pressure[10]. The pressure was applied to each valve for 3 trials of 5minutes and the amount of water that leaked through the valve was measured. The volume of water leaking from the valve was collected using a recipient placed under the assembly. After each trial, the recipient was weighed to determine the volume of the water collected. The second test consisted of pushing the lead through each valve and measuring the peak force required. This measurement was taken 5 times for each valve.

Figure 43: Valve testing setup

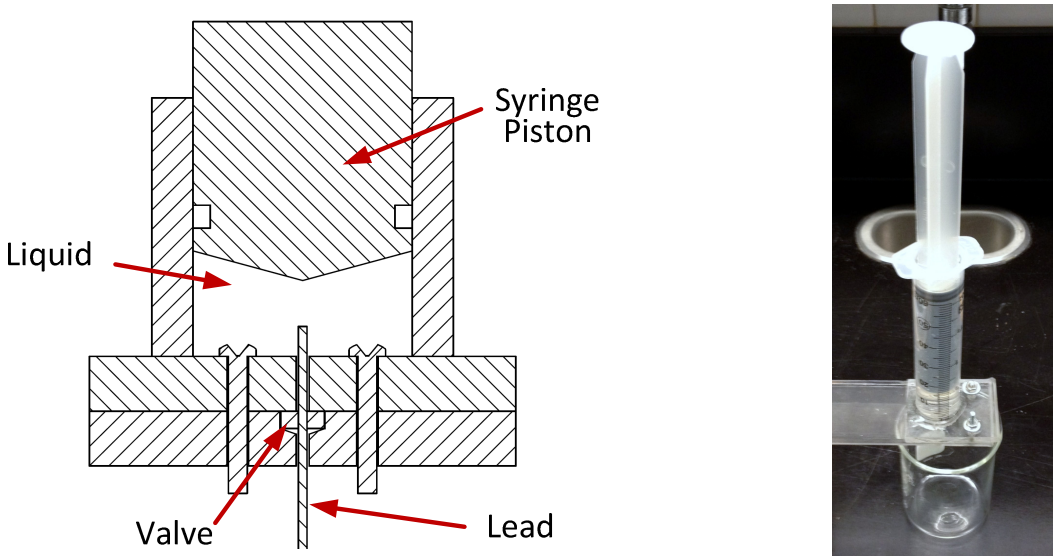

[10] Blood pressure of 200mm of Hg can be found in arteries but not in large veins. Blood pressure in veins such as SVC and subclavian veins is usually below 10mm of Hg. Therefore, using 200mmHg represents a safety factor of about 20.(Human Physiology: An Integrated Approach, 4th Edition, p.505)

The results of both tests are as follows:

Table 11: Valve leak and push force results summary for Prototype 3

	Valve #1 (Ø0.80mm)	Valve #2 (Ø1.38mm)	Valve #3 (Ø1.60mm)
Leak Volume (ml)	No leak	3.67 ±0.58	7.67 ±1.53
Push Force (N)	4.94 ±0.17	0.86 ±0.07	0.33 ± 0.03

6.3.3. Data Analysis

6.3.3.1. Noise protection test

Without noise, the system showed a peak-to-peak amplitude which is equivalent to a 0.03mm oscillation (2mV), while with the worst-case noise, the system could be seen oscillating for a full 0.3mm (20mV). With 1mm displacement being equivalent to a 67mV change in signal, 20mV has the potential to induce an oscillation of the last significant digit.

Noise cancelation using a capacitor bypass on the power supply did not achieve any reduction in noise. In these conditions, bypassing the power supply to the ground reference using a capacitor did not reduce the peak-to-peak amplitude of the signal significantly. However, by applying the capacitor bypass to the signal rather than the power supply, the amplitude of the noise was reduced by nearly 20% from approximately 21mV to 17mV peak-to-peak. This reduction is thought to originate from the filtering of the electrical noise absorbed by the linear potentiometer. Since a majority of the noise was still reflected by the signal, a different setup was tested by placing the capacitor bypass on the end of the cable that is proximal to the data acquisition system. This configuration produced a signal with an amplitude comparable to the original unfiltered signal, with no noise. The result, therefore, showed that the majority of the noise absorbed by the system originated from the length of cable used to link the system to the data acquisition system. With and without being exposed to artificial environmental noise, the signal remained within 2mV of peak-to-peak amplitude.

6.3.3.2. Valve Test

All three valves managed to fulfill their role effectively. Valve #1 did not let any water through during its testing. Water did leak through both valve #2 and #3. However, the volumes of water were consistently low, never being higher than 10ml, which should be considered as satisfactory considering the high safety factor used for determining the blood pressure used.

The force required to move the lead through valve #1 was much higher than the maximum force of 0.75N set in the requirement. The other two valves allowed much easier movement of the leads with forces below 1N. However, the force necessary to move the lead through valve #2 was still higher than the requirement. Valve #3 was the only one with results which complied with the force requirement. In fact, if it were to be assembled in series with Prototype 2, and the force required to move the lead were to be added, the force would still remain lower than 0.75N (Total of 0.48N). It should be noted that the valve through-hole that produced the best result was made using a tool with a diameter larger than the lead it was made for (1.68mm > 1.30mm). An inspection of the valves under a microscope suggests that the valve was only stretched by the tool, and not permanently deformed to the diameter of the tool. Otherwise, the through-hole would have been larger than the lead, which should have resulted in a significantly larger leak.

6.3.4. Discussion

Apart from the problem with the surface finish, some other problems related to the prototype's usability were noticed.

By correlating the results of the valve test with the results of the Flexipot sensor testing when immersed in water, one can theorize that all three valves would serve as a sufficient barrier from blood. Considering the sensor can withstand total immersion for a few hours, the impact of a few millilitres of blood over hours should not affect its performance. Additionally, blood, unlike water, is likely to coagulate around the valve, thus quickly improving its performance. However, a significant amount of resistance was also added by all valves. Nevertheless, valve #3 still managed to prove that it was possible for a valve to find a good trade-off between a good seal and low resistance. Using larger through-holes could also be possible considering the large safety factor that was applied to the test. In this case, resistance to movement would likely be lower.

To verify the claim that the noise originated from the cables, it was possible to test the system's responsiveness to noise by isolating the cables from the problem. To test this, the cable was wrapped in a foil shield (a very effective way to protect a system from noise contamination). The test was then repeated using the same source of artificial noise. Figure 44 shows the influence of noise on the trace. The peak-to-peak amplitude of the signal with this

configuration was 3.9mV. This confirms that approximately 90% of the noise can be suppressed by better shielding the cables.

Figure 44: Noise Suppressed Using Foil Shielding Over Cables

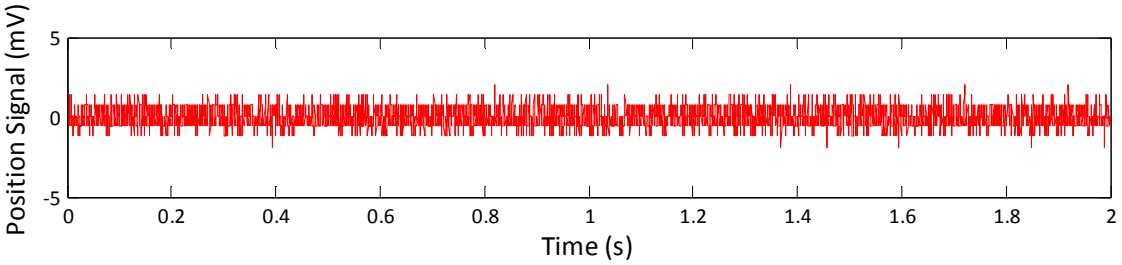

Lastly, the PolyJet 3D printing process did not yield the same quality of surface finish for Prototype 3 as it did for Prototype 2. The surface finish of the important sliding surfaces was considerably rougher than those of Prototype 2. Considering that 3D printers have different resolutions for different axes, the parts were presumably not produced in the same orientation. In the future, this could probably be avoided by asking for a specific orientation where the planeity and surface finish of the most important surfaces would be maximized, or by simply switching to a different manufacturing process that allows for more control.

Although Prototype 3 did not yield pre-clinical results in its intended use, it allowed for refining of the concept that was already confirmed as adequate by the previous prototype. The changes suggested in this section should therefore be applied, in the future, to the clinical version which should be adapted to a certified biocompatible material and manufacturing process.

7. Recommendations

Through three iterations of prototypes, many lessons were learned and many things were achieved, and each prototype helped show better ways to fulfill the previously established requirements. Table 12 summarizes the best results accomplished by the prototypes described in this thesis.

Table 12: Summary of requirement fulfillment

Requirement	Level	Best Result	Comments
Linear Travel	50mm	60mm *(Prototype 2)*	Achieved by one side of the prototype.
Angular Travel	360deg	360deg *(Prototype 1/2)*	Achieved with variable smoothness of movement.
Linear Position Accuracy	±1.00mm	±0.15mm *(Prototype 2)*	Average accuracy of Prototype 2, with the worst error as 0.30mm.
Linear Position Repeatability	±1.00mm	±0.04mm *(Prototype 2)*	Average repeatability of Prototype 2, with the worst result as 0.06mm.
Push/Pull Force	0.75N	Average of 0.15N *(Prototype 2)*	A 0.33N resistance was achieved using a valve designed for Prototype 3.
Fatigue	50 Cycles	Passed *(Prototype 2)*	Performed 50 cycles of fatigue testing and beyond 40 more cycles for other tests.

However, some elements also emerged during testing and through the evolving context of the project. These aspects can mostly be addressed by looking at the constraints previously defined.

Table 13: Lessons learned relative to the project's constraints

Constraint	Comments
Intuitive control of electrodes	No change to the method used to move electrodes was introduced by adding the positioning system. The conventional way of moving intravascular lead can then be used by therapist.
Prolonged use	MRI compatibility was not tested using the prototypes presented in this document but none of the metal parts used displayed any magnetic properties.

Fixed reference frame	As explained for Prototype 3, the system should be permanently associated with the lead system and to the body so that the reference frame is truly reliable.
Digital acquisition of position	Noise has been observed while acquiring position data. However, mitigation is possible using cable shielding and signal filtering.
Maintain safety and functionality in a clinical setting	The protection of the system from the influence of other equipment has been shown using filtering, while protection from fluids has been shown using the addition of a valve at the interface with the body.
Allow sterilization	Rapid prototyping allows sterilization, however limited data is available relative to the behavior of the 3D printing materials when used in medical systems where biocompatibility is necessary.

With this information in mind, it is possible to examine the different ways to include all of these solutions into one prototype. Additionally, considering the scope of an academic thesis, some manufacturing processes remained out of reach; therefore, some ideas could never be truly implemented. The following section aims to outline possible embodiments that this positioning system could take in order to bring this concept to a marketable product.

7.1. Material and Manufacturing Process

Although 3D printing is a powerful tool when building prototypes, it is not entirely adequate to use in a future commercial or clinical setting. First and foremost, this process is ideal for producing limited numbers of unit but is not cost-effective for larger numbers. Second, products used in a clinical environment need to abide by the ISO-10993 biocompatibility standard.

With its small batch sizes and great versatility with no initial tooling investment, rapid prototyping is an ideal choice for production of a few units. However, these same elements also make the process ill-adapted to larger productions. The unit-price of parts built with 3D printing does not reduce with larger quantities. The only price reduction comes from the short set-up cost which is shared over by the units being made in a single run. In comparison, processes like injection moulding require a large initial investment but are then built at a low unit cost.

Another consideration in terms of materials is that according to the ISO-10993 standard, “external communicating devices” with an access to the vascular system must pass a series of tests. Those tests are as follows:

- Cytotoxicity, where the material is tested for its capacity to cause cell death or stop cell growth.
- Sensitization, where the material is tested for its ability to elicit an allergic reaction.
- Intercutaneous reactivity, where the material's potential to generate skin irritation and other skin damage is tested.
- Acute toxicity, where the material is tested for its potential to release toxic waste into the body.
- Haemocompatibility, refers to the material's interaction with the patient's blood.

Such tests may not be necessary in all situations, especially if the material can be shown to have a significant history under comparable conditions. However, demonstrating such history can be complex since companies do not willingly divulge the composition of their products and the manufacturing processes used.

For example, although materials such as the ABS-M30i and PC-ISO are said to be certified according to the biocompatibility standard and said to be in use in medical devices[11], the 3D printing processes used to shape those materials are not publically certified. Therefore, using those processes would involve large expenses to perform the testing mentioned above. Therefore, it would be wise to use commonly available materials with a documented history under standard manufacturing processes, such as injection moulding and machining.

7.2 Custom Membrane Potentiometer Concept

Although the prototypes described in this thesis offered good performance, there is still much room left for improvement. Some of the main faults of the previous prototypes included the lack of a proper referencing of the position, and the size of the housing. Integration of the sensor into a custom made commercial catheter-lead system would solve of both problems. In doing so, the catheter could be made to include the membrane potentiometer sensors and the beads directly within the hub.

[11] From Proto3000, 3D engineering solution, official website: *http://www.proto3000.com/rapid-prototyping.aspx?topidcol=7*, October 9th, 2011.

To produce such an embodiment of the position sensor and stimulation leads, the complete system would have to be custom made. A custom hub would ideally be molded around the sensing elements to produce a more integrated solution, which unlike previous prototypes, would not allow the user to access the inside of the system and potentially introduce contaminants. The hub necessary to house such a sensor would need to be significantly longer than regular catheter hubs. Common intravascular catheters use a hub with a flat triangular shape about 20 to 30 mm long and 5 to 8 mm thick[12]. Assuming a minimum electrode travel of 50mm, it is obvious that a special hub would need to be manufactured.

Hypothetically, the system could use a sensor with an active region shorter than 50mm. The potentiometers could be positioned in the same back to back configuration used in previous prototypes, however, by using a sensor of custom geometry, the width of the sensor (outside it its active area) could be reduced to minimize the thickness of the hub. Currently the sensor spans 11.6mm, while the width of the active region is only 4.3mm, leaving 3.65mm for each support side. Assuming a slight miniaturization, the widths could be reduced to 2.5mm for the active region and 2.0mm for each support side. The guide could then be molded directly into the hub to fit the bead and sensor.

Figure 45: Theoretical custom membrane potentiometers shape and position

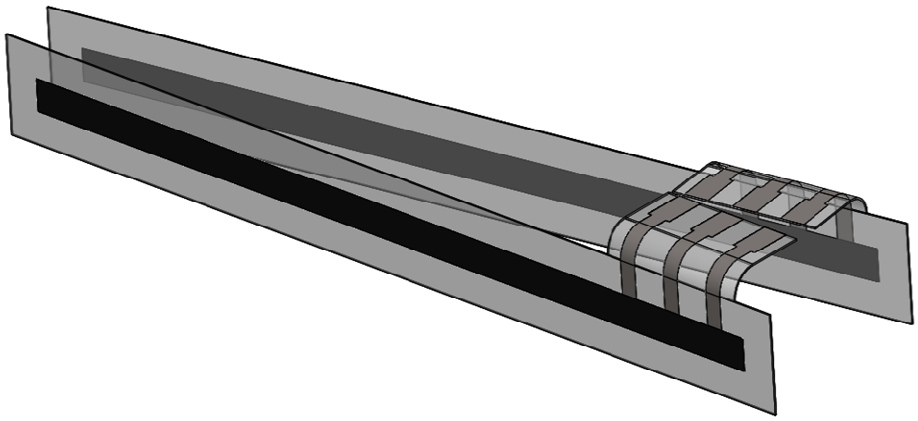

[12] These measurements are inspired from measuring a few different catheters, and do not necessarily represent the entire market of intravascular catheters. Indeed, some catheter systems don't have any hub with suture tabs.

By using a customized membrane potentiometer, it would also be possible to reposition the contacts. To save space, the connection contacts could be repositioned to the side of the sensor, at the end proximal to the therapist. By placing the potentiometers back to back, an area would be left unused where the sensors are most spread apart. This area could potentially be used to house the connection to the sensors. This area could also easily be used to route a strain-relieved cable, or connector to link the sensor to the control unit. This customization could also be used to add a capacitor directly into the circuit of the potentiometer. The signal would therefore be automatically smoothed and assembly would be simple.

The hub's material should be chosen to comply with two criteria: low friction coefficient and relatively high stiffness. First, to allow proper sliding of the bead on the guide, as explained previously, the material needs to have a low coefficient of friction[13]. Second, the material will have to be stiff enough to limit possible deformation of the hub. Although reliable, membrane potentiometers are likely to produce erroneous signals when they are deformed along their active region, as explained in section 5.1.4. Multiple other criteria will also have to be taken in consideration when designing the hub. Amongst them, the hub's material shall need to allow easy integration with the catheter shaft, and the material chosen shall need to have appropriate chemical properties certified not to react with any injectable medicine.

As it was mentioned previously, one way to manufacture a hub fitted with position sensors is to have the sensors be included into the mould itself. This way the plastic is formed around the sensors, thus securing them in place permanently. However, due to their low tolerance to high temperatures, the sensors are unlikely to endure such a harsh assembly. Alternatively, another method could potentially be used, in which a mould is used in concert with mandrels to form pockets inside a plastic parts. In such cases, the mandrels are machined to correspond to the empty space meant to remain in the plastic part after moulding. In other words, they are placed into the mould and plastic is shot around them. After the plastic has all been injected, the mandrels are pulled out, leaving an imprint of their shape. The mandrels are

[13] With Teflon having a dynamic coefficient of friction of about 0.10, materials with coefficients of friction up to 0.20 would be suitable. Such materials include UHMV, PEEK, and Delrin.

generally tapered to make them easier to remove. Other strategies include Teflon coatings and other surface finished. Mandrels are commonly used in catheters to create lumens in catheters hubs. The same strategy is illustrated in the following figure.

Figure 46: Moulding over mandrels, (A) mandrels only, (B) mandrels with plastic molding over them, (C) without mandrels, final assembly

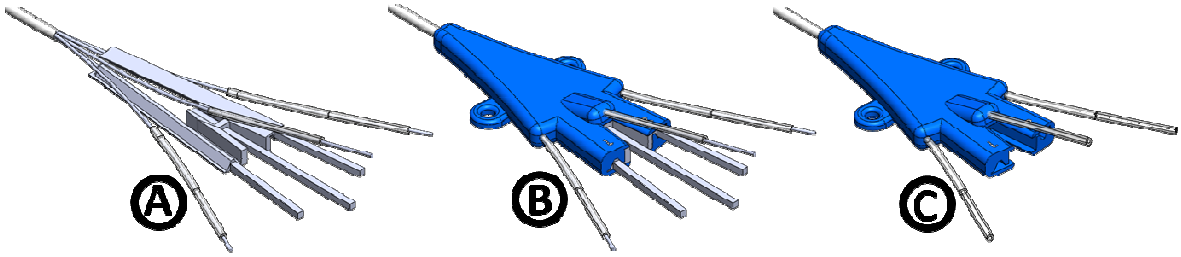

The addition of a thin polymer membrane to improve the bead's contact would also cause difficulties because of the temperature restrictions. A potential cost-saving solution would be to include a narrow trough along the surface on which the sensors rest. By minimizing the thickness of this surface, the sensor would be able to recede by a fraction of a millimetre at its point of contact with the bead. This pocket would then act in the same way as the polymer. However, this solution would have to comply with the chosen manufacturing process. If the part is moulded in one piece, the slit would have to extend to the edge of the part to allow the support material to be removed. In the instance where the hub is made from two different parts, the FlexiPot sensor and a polymer membrane could be inserted inside the structure before fixing the two halves of the hub together. This depends, though, on the properties of the plastic used for the hub.

To insure that the sensors are fixed in a reliable reference frame, the catheter hub can be sutured to the skin of the patient as is typical for IVCs. By having the hub fixed to the skin, the position of the sensors relative to the nerves would always remain the same unless the body moves and the whole catheter is pulled or pushed. In practice, whenever a patient is moved, he/she will be moved back to the original position and it is reasonable to assume that the catheter would also return to its original position if the hub remained sutured to the skin..

In summary, for the concept described above to fit in a catheter hub, the hub would need to have approximate dimensions of 35 mm wide, 70 mm long, and 9 mm thick. Figure 47a shows a conceptual drawing of a 5 lumen hub with 2 lumens housing leads, and 3 lumens used

for fluid delivery. The conceptual hub also shows the suture tabs necessary to fix its position. On the right hand side, Figure 47b shows the same catheter sitting on a modelled chest.

Figure 47: Conceptual representation of a position tracking catheter hub

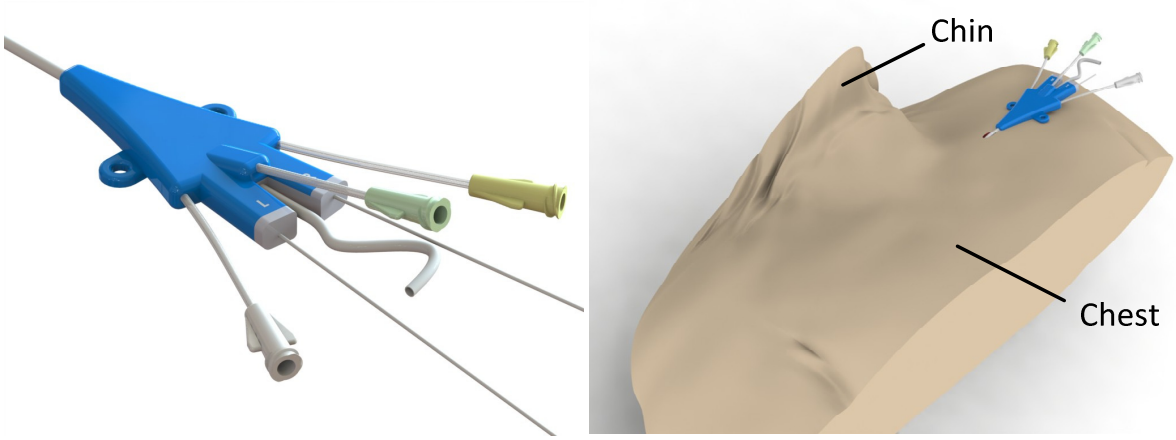

(a) ***(b)***

8. Summary and Conclusions

The efficiency and stability of transvascular neurostimulation is greatly dependent on the proximity of the electrodes to their target nerve. Therefore, an important aspect of neurostimulation therapy is the positioning of electrodes. With the only positioning method previously available to the Neurokinesiology Lab hinging on manual ruler measurements, it was necessary to design a positioning sensor that would keep track of each electrode's position precisely and automatically. Such a sensor would help to reduce mapping time by allowing a control unit to correlate stimulation efficiency with electrode position.

To achieve these objectives, a few iterations of inexpensive intuitive sensing units were designed and built. To keep track of electrode position, the positioning system is fitted to the intravascular leads between their insertion point into the body and the proximal ends controlled by the therapist. Within the housing, linear membrane potentiometers allow a control unit to derive position from a variable resistance. Using this concept, a repeatability of ±0.06mm was achieved with an average accuracy level of ±0.19mm even after a significant amount of use. Additionally, the use of this system has been shown to add a small amount of resistance to the movement of the leads with a force of less than 0.75N to move the lead within the system.

This solution is both mechanically simple and fairly inexpensive. With two membrane potentiometers available off the shelf for less than $30, a custom injection molded housing for under $5 (when produced in large quantities), and all other parts totalling under $10, this design allows a relatively inexpensive, disposable solution to the positioning problem.

Some additional elements would have to be modified in order to integrate this concept into a commercial clinical product. The changes in question would refer to the material choice and the shape of the housing. For example, the positioning sensors could be molded directly into a catheter hub making it invisible to the therapist. In this form, the system would also allow for continuous monitoring of the position by being permanently associated with the electrode leads.

Obviously this positioning system could have taken many other shapes. However, considering the scope of a Master's thesis project, the solution proposed within this document manages to remain elegant, inexpensive, simple, and intuitive to a therapist.

References

Arai, F., Fujimura, R., Fukuda, T., Negoro, M., New Catheter Driving Method Using Linear Stepping Mechanism, in Proc. IEEE Int. Conf. Robotics and Automation (ICRA 2002), Washington, DC, 2002, pp. 2944–2949.

Da L, Zhang D, Wang T., Overview of the vascular interventional robot, Int J Med Robot. 2008 Dec;4(4):289-94.

Dasta, J. F., McLaughlin, T. P., Mody, S. H. and Piech, C. T., Daily Cost of an Intensive Care Unit Day: The Contribution of Mechanical Ventilation. Critical Care Medicine, 2005, 33(6), 1266-1271.

DiMarco, A.F., Connors, A.F., Jr., and Kowalski, K.E., Gas exchange during separate diaphragm and intercostal muscle breathing, J Appl Physiol 2004, 2120-2124.Dreyfuss, D., Saumon G. (1998). Ventilator-induced lung injury: lessons from experimental studies. Am J Respir Crit Care Med; 157(1):294–323.

Esteban, A et al., How Is Mechanical Ventilation Employed in the Intensive Care Unit?, Am. J. Respir. Crit. Care Med., Volume 161, Number 5, 1450-1458, May 2000.

Esteban A., Anzueto A., Frutos F., Alia I., Brochard L., Stewart T.E., Benito S., Epstein S.K., Apezteguia C., Nightingale P., Arroliga A.C., Tobin M.J., Characteristics and Outcome in Adult Patients Receiving MV. The Journal of the American Medical Association, 2002, 287(3), 345-355.

Fell, S.C., Surgical Anatomy of the Diaphramg and the Phrenic Nerve, Chest Surgery Clinics of North America, Vol 8, Issue 2, 281-294.

Fragou, Mariantina; Gravvanis, Andreas; Dimitriou, Vasilios; Papalois, Apostolos; Kouraklis, Gregorios; Karabinis, Andreas; Saranteas, Theodosios; Poularas, John; Papanikolaou, John; Davlouros, Periklis; Labropoulos, Nicos; Karakitsos, Dimitrios, Real-time ultrasound-guided subclavian vein cannulation versus the landmark method in critical care patients: A prospective randomized study, July 2011, Vol39, Issue 7, 1607-1612.

Frisch, S. (2009). A Feasibility Study of a Novel Minimally Invasive Approach for Diaphragm Pacing Simon Fraser University, Confidential MSc Thesis, under Dr. Hoffer's supervision.

Gelfand, M., Levin, H.R., Halpert, A., System and method to modulate phrenic nerve to prevent sleep apnea, US Patent Application, 11/601,150, filed Nov 17, 2006.

Glenn, W. W. L., Hogan, J. F., Loke, J. S. O., Ciesielki, T. E.; Phelps, M. L., Rowedder, R., Ventilatory Support by Pacing of the Conditioned Diaphragm in Quadriplegia. Survey of Anesthesiology, August 1985, Vol29, Issue 4, 209.

Gray, H., Anatomy of the Human Body. Philadelphia: Lea & Febiger, 1918; Bartleby.com, chapter 6.4, 2000. www.bartleby.com/107/

Groves, D.A., Brown, V.J., Vagal nerve stimulation: a review of its applications and potential mechanisms that mediate its clinical effects, Neuroscience & Biobehavioral Reviews Vol29, Issue 3, May 2005: 493-500.

Hansen-Flaschen, J.H., Brazinsky, S., Basile, C., Lanken, P.N., Use of Sedating Drugs and Neuromuscular Blocking Agents in Patients Requiring Mechanical Ventilation for Respiratory Failure, Journal of American Medical Association, 1991;266(20):2870-2875.

Guo S, Kondo H, Wang J, et al. A new catheter operating system for medical applications. Proceedings of the 2007 IEEE/ICME International Conference on Complex Medical Engineering; 23–27 May 2007; 111–115.

Hoffer, J.A. Transvascular Nerve Stimulation Apparatus and Methods. US Patent Application 60/887031, filed 29 Jan 2008.

Hoffer JA, Tran BD, Tang JK, Saunders JTW, Francis CA, Sandoval RA, Meyyappan R, Seru S, Wang HDY, Nolette MA, Tanner AC. Diaphragm Pacing with Endovascular Electrodes. IFESS 2010 - Int'l. Functional Electrical Stimulation Soc., 15th Ann. Conf., Vienna, Austria, pp 40-42, 2010.

Ingfei Chen, In a World of Throwaways, Making a Dent in Medical Waste, New York Times, July 6th 2010, page D1.

Ishii Kiyoshi, Kurosawa H, Koyanagi H, Nakano K, Sakakibara N, Sato I, Noshiro M, Ohsawa M., Effects of bilateral transvenous diaphragm pacing on hemodynamic function in patients after cardiac operations, J Thorac Cardiovasc Surg. 1990 Jul;100(1):108-14.

Khong, P., Lazzaro, A, Mobbs, R., Phrenic nerve stimulation: The Australian experience, Journal of Clinical Neuroscience 17 (2010) 205–208.

Kress, J.P., Pohlman, A.S., O'Connor, M.F, and Hall, J.B., Daily Interruption of Sedative Infusions in Critically Ill Patients Undergoing Mechanical Ventilation, N Engl J Med 2000; 342:1471-1477.

Lambert, BJ, Tang FW, Rationale for practical medical device accelerated aging programs in AAMI TIR 17, March 2000, Volume 57, Issues 3–6, pp. 349–353.

Lemaire, F., Difficult weaning. Intensive Care Medicine, 1993, 19, S69 - S73.

Levine, S., Nguyen, T., Taylor, N., Friscia, M.E.,Budak, M.T., Rothenberg, P., et al. (2008). Rapid Disuse Atrophy of Diaphragm Fibers in Mechanically Ventilated Humans. The New England Journal of Medicine 358(13): 1327-1335.

MacIntyre, N.R., Evidence-Based Guidelines for Weaning and Discontinuing Ventilatory Support, CHEST December 2001 vol. 120 no. 6 suppl 375S-396S.

Merrer J, De Jonghe B, Golliot F, Lefrant JY, Raffy B, Barre E, Rigaud JP, Casciani D, Misset B, Bosquet C, Outin H, Brun-Buisson C, Nitenberg G, Complications of femoral and

subclavian venous catheterization in critically ill patients: a randomized controlled trial., JAMA. 2001 Aug 8;286(6):700-7.

Mitsutaka Tanimoto, Fumihito Arai, Toshio Fukuda, and Makoto Negoro, "Augmentation of Safety in Teleoperation System for Intravascular Neurosurgery", Proceedings of the 1998 IEEE International Conference on Robotics & Automation, pp.2890-2895, Leuven, Belgium, May 1998.

Naylor, Christine L, Reduction of Malposition in Peripherally Inserted Central Catheters With Tip Location System, Journal of the Association for Vascular Access, Spring 2007, vol12-1, pp. 29-31(3).

Onders Raymond P., Elmo M.J., Ignagni, A.R, Diaphragm Pacing Stimulation System for Tetraplegia in Individuals Injured During Childhood or Adolescence, J Spinal Cord Med. 2007; 30(Suppl 1): S25–S29.

Paraskevas, G. K., Raikos, A., Chouliaras, K. and Papaziogas, B., Variable anatomical relationship of phrenic nerve and subclavian vein: clinical implication for subclavian vein catheterization. British Journal of Anaesthesia 106 (3): 348–51, January 2011.

Perna F, Heist EK, Danik SB, Barrett CD, Ruskin JN, Mansour M., Assessment of Catheter Tip Contact Force Resulting in Cardiac Perforation in Swine Atria Using Force Sensing Technology, Circ Arrhythm Electrophysiol. 2011 Apr;4(2):218-24.

Sassoon, Catherine S. H., Ercheng Zhu and Vincent J. Caiozzo, Assist–Control Mechanical Ventilation Attenuates Ventilator-induced Diaphragmatic Dysfunction, American Journal of Respiratory and Critical Care Medicine Vol 170. pp. 626-632, (2004).

Sieck, Gary C., and Carlos B. Mantilla, Effect of Mechanical Ventilation on the Diaphragm, N Engl J Med 2008; 358:1392-1394, March 27, 2008.

Tang, Jessica, Modeling the Requirements for Selective Phrenic Nerve Activation with Intravascular Electrodes, Simon Fraser University, 2009.

Tang, Jessica, and Joaquin Andres Hoffer, Transvascular electrode model and stimulation parameter estimation. Canadian Medical and Biological Engineering Conference, Burnaby,BC, 2010.

Tripathi, Mukesh,and Tripathi, Mamta, Subclavian vein cannulation: An approach with definite landmarks, The Annals of Thoracic Surgery, January 1996, Vol61, Issue 1, 238–240.

Appendices

Appendix A

Seldinger Technique for Insertion of LIVE Leads

To understand how the LIVE assembly is introduced in the vein of a patient, it is important to first understand the Seldinger technique. The following steps and pictures[1] explain the method used by the Neurokinesiology team for insertion of IV electrodes.

Figure 48: Step by step procedure of the Seldinger technique adapted to the insertion of LIVE leads

1. Once the vein is located, using visual landmarks or ultrasound, a needle is inserted percutaneously and blood is withdrawn to confirm position.

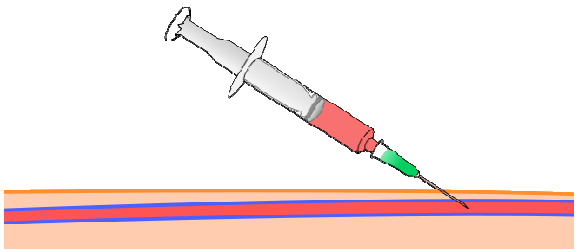

2. A guidewire is threaded through the needle and into the vein.

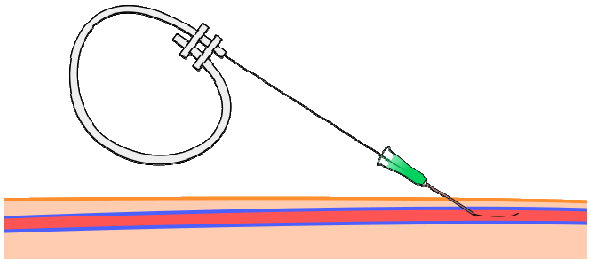

3. The needle is removed.

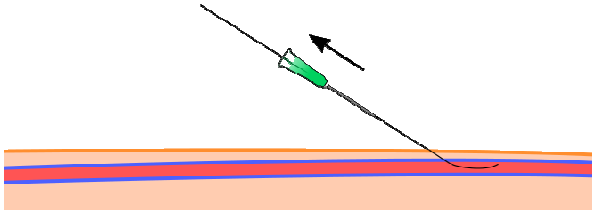

4. A dilator (blue) fitted with an introducer (yellow/gray) is inserted over the guide wire. The guide wire can then be removed.

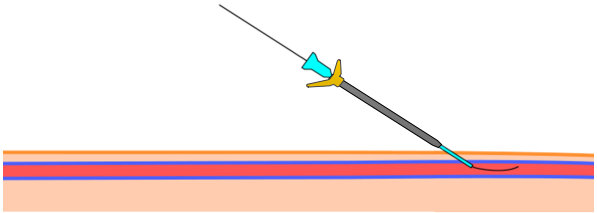

5. Once the introducer and dilator are in, the dilator is removed and only the introducer is left. A catheter or in this case, the intravascular electrodes, can now be inserted into the introducer.

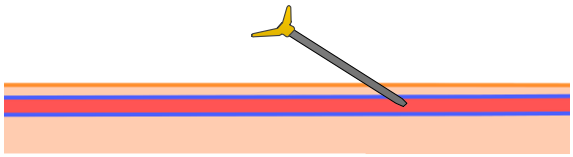

---

[1] Pictures modified from http://en.wikipedia.org/wiki/Seldinger_technique.

Appendix B

Electrode Orientation for Phrenic Nerve Stimulation

As it was explained in section 1.1.4, to find the best stimulation parameters the electrodes have to be positioned as close as possible to the nerve while facing it. In theory, one could try stimulating at every depth and every angle to find which depth and orientation yields the best results, however, to minimize mapping time the number of orientations to explore can be reduced to one for each nerve.

Figure 49: Ideal electrode orientation for stimulating the left phrenic nerve (yellow) crossing from the subclavian vein (red)

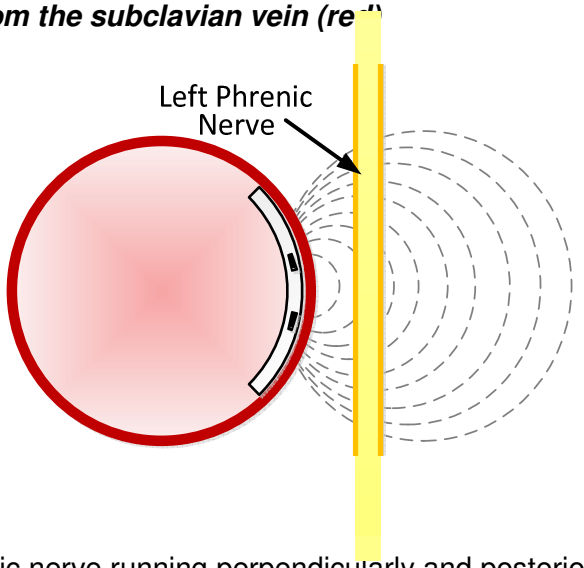

With the left phrenic nerve running perpendicularly and posteriorly to the subclavian vein as shown in Figure 49, the best electrode angle for stimulation of this nerve is undoubtedly the posterior orientation. The nerve cannot be expected to cross above or below the subclavian vein, since the nerve's trajectory is known to be nearly vertical, pointing towards the diaphragm [Gray, 1918]. As for the nerve crossing anteriorly to the vein, it been reported as a rare occurrence [Paraskevas et al. 2011]. Assuming that the main branch of the phrenic nerve provides the majority of the neural drive to the diaphragm, stimulation in the posterior orientation would still remain effective.

Figure 50: Simplified representation of the path used by the right lead electrode to reach the optimal site for stimulation of the right phrenic nerve

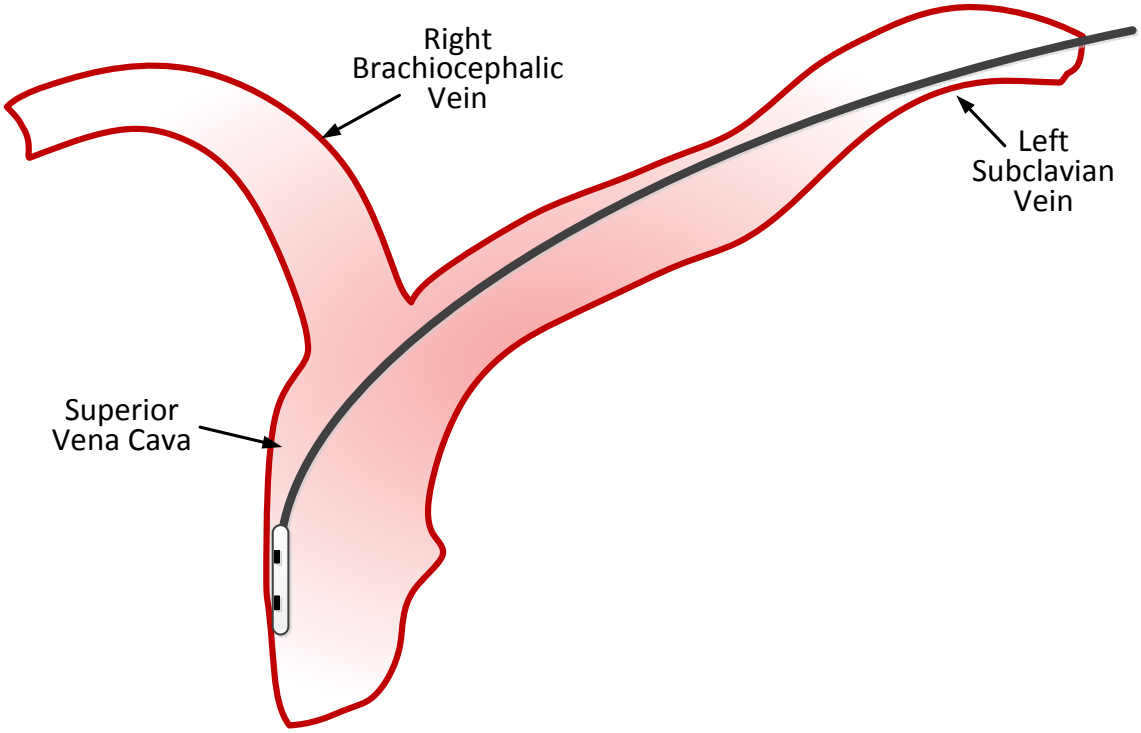

In the case of the right phrenic nerve, the precise orientation at which stimulation is ideal could potentially vary since the nerve runs parallel to the superior vena cava. The right phrenic nerve is expected to be very close to the vessel wall as it makes its way caudally along the side of the heart to the diaphragm. For this reason, the nerve should lie lateral to the superior vena cava with some anterior or posterior variability. However, varying the orientation of the electrode in the vein to stimulate the right phrenic nerve at a precise orientation may not be as simple. By using a flexible lead that conforms to the bend of the vasculature, as shown in Figure 50, the electrodes are constrained by their contact to the far right side of the vessel. A lead flexible enough to not risk puncturing a vessel wall, rotation of the lead, at the proximal end by the therapist is unlikely to produce a proportional rotation at the distal end. Instead, rotation at the proximal end of the lead may not produce sufficient rotation at the distal end, and if it does, the rotation that ensues may not be smooth, reproducible, or proportional to the rotation of the proximal end. Instead, it may get caught in the vessel wall, or move jerkily when the lead is rotated sharply. Another risk of such a rotation is that the lead may rotate on its own axis thus exposing the electrodes to blood flow instead of being in contact with the vessel wall.

Figure 51: Rotation of the lead electrode as it is being pushed against the far side of the superior vena cava exposing the electrode to the blood flow

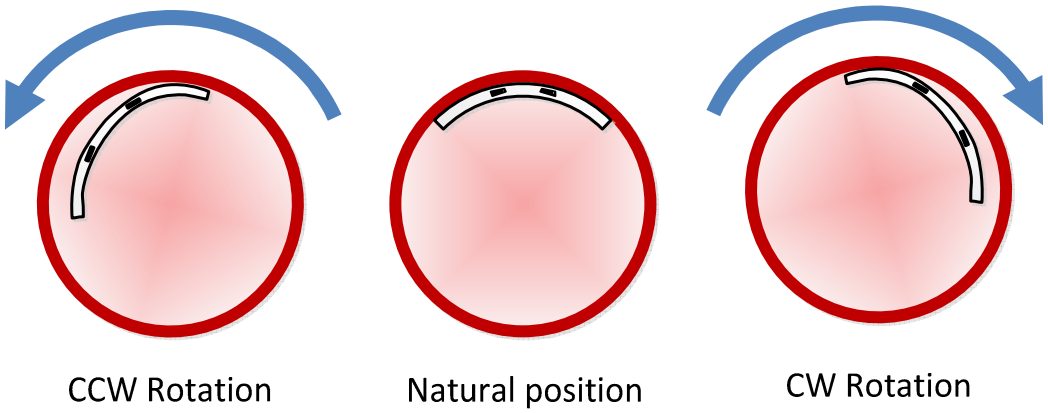

For the reasons explained above, the natural orientation of the right array electrode array in the superior vena cava is the only orientation that can reliably be used. Variation in the position of the nerve in the anterior and posterior directions should therefore be covered by other means such as, for example, a distribution of electrodes in a wider electrode array

In summary, both stimulation sites offer only one orientation in which stimulation is likely to occur, and it may be difficult to rotate an electrode array precisely when in the superior vena cava. Although, the latter restriction will need to be experimentally documented in future animal trials.

Appendix C

3D Printing Processes and Materials

The table below shows the more relevant 3D printing processes offered by the company Quickparts on their website.

Table 14: QuickParts Process Comparison

	Stereolithography (SLA)	PolyJet		Selective Laser Sintering (SLS)	Fused Deposition Modeling (FDM)
		Tango	Vero		
Instant Quoting Maximum Dimensions	25" x 25" x 21"	19.3" x 15.4" x 7.9"	19.3" x 15.4" x 7.9"	28" x 19" x 19"	ABS: 23" x 19" x 23" Polycarbonate: 14" x 16" x 16"
Layer Thickness	High-Resolution: 0.002" - 0.004" Standard Resolution: 0.005" - 0.006"	Horizontal build layers down to 16 microns (0.0006 inches)		Standard Resolution: 0.004"	Standard Resolution: 0.01"; Minimum wall thickness is 0.02"
Material Options	ABS-Like White (Standard & High Res), ABS-Like Gray, ABS-Like Black, Rigid PC-Like (Standard & High Res), Durable PP-Like (Standard & High Res), Semi-Flexible PE-Like, High-Impact ABS-Like, High-Temp ABS-Like, High-Temp PC-Like, Rigid, & Technician's Choice	Elastomeric: 61A Tango Black, 75A Tango Gray, & Rubber-Like Tango Plus	High Res Rigid VeroTranslucent, High Res Rigid VeroBlue, High Res Rigid VeroBlack & High Res Rigid VeroWhite	Nylon, Glass-Filled Nylon, Durable Nylon, & Flame-Retardant Nylon	ABS, ABS-M30, ABSi, PC-ABS, ABS-M30i, PC-ISO, Ultem, PPSF & Polycarbonate
Finish Options	Strip & Ship, Standard, Primed, Painted, WaterClear, & Nickel-plated	Standard Finish Only		Standard finish rougher than SLA due to base material being a powder.	No special finishing due to toughness of material.
Lead Time Options	Same Business Day Shipment, Next Business Day Shipment, # of Business Days from Order Date	Standard (3 - 5 Days)		Next-day shipment, Standard (3 - 5 days), Economy (8 - 10 days)	Standard (3 - 5 days)
Recommended Minimum Feature Size	High-Resolution: 0.010" - 0.015" Standard Resolution: 0.025" - 0.035"	0.045"	0.025"	0.030" - 0.040"	0.025"
Quoted Price for 2nd Prototype	High-Resolution: 952$ Standard Resolution: 574$	514$	368$	392$	576$

* Table taken from Quickparts.com and last row added using their online quoting service.

PolyJet is a 3d printing process that uses UV photopolymer and support material. Using the Vero materials, the standard tolerances are of ±0.005" for the first inch, and +/- 0.002” on every inch thereafter for dimensions in the horizontal plane, while dimensions in the vertical axis axis obeyed to tolerances of +/- 0.01" for the first inch, +/- 0.002” on every subsequent inches. The 3 families of Vero PolyJet materials offer very similar properties, therefore the Rigid VeroWhite was used. The color white was strategically chosen to show where blood would infiltrate the housing.

Table 15: Hi Res Rigid VeroWhite, VeroBlack Material properties

Mechanical Properties	Tensile Strength	Tensile Modulus	Tensile Elongation at Break	Flexural Strength	Flexural Modulus	Hardness	Izod Impact - Notched	Heat Deflection Temp
Test Method	ASTM D638	ASTM D638	ASTM D638	ASTM D790	ASTM D790	DIN 53505/2240	ASTM D256	ASTM D648
Units	psi	Psi	%	psi	psi	Shore	(ft-lb)/in	°F
High Res Rigid Translucent (FC720)	6,100	N/A	15-25%	10,200	286,800	N/A	0.5-0.7	110-115
High Res Rigid VeroBlue (FC840)	7,900	N/A	15-25%	12,100	287,600	N/A	0.8	113-120
Hi Res Rigid VeroWhite, VeroBlack	7,200	N/A	15-25%	10,800	309,900	N/A	0.7	113-120

Appendix D

First Prototype Information Summary

This section contains additional relevant information about Prototype 1 not disclosed in the thesis body.

Table 16: First prototype information summary

Categories	Information
Weight	25g
Process	Off the shelf parts materials and parts cut down to customized with basic tooling.
Materials	PTFE, Acrylic, 18-8 Ss Button Head Socket Cap Screw, 0-80 Thread, 1/8" Length
Other information	Used instant adhesive Loctite XXX for fixation of parts.

Figure 52: Important dimensions of first prototype (dimensions in mm)

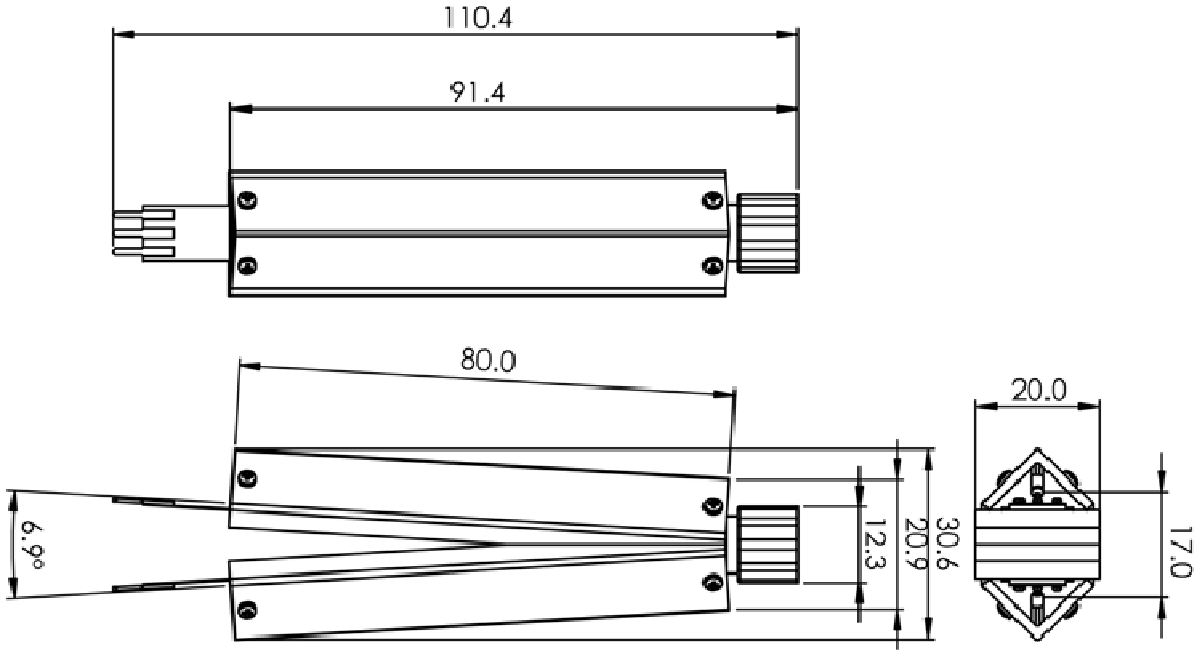

Appendix E

Second Prototype Information Summary

This section contains additional relevant information about Prototype 2 not disclosed in the thesis body.

Table 17: Second prototype information summary

Categories	Information
Weight	45g
Process	PolyJet
Materials	Hi-Res VeroWhite, Stainless Steel Hypotube
Other information	Made to mate with Greatbatch 12Fr Introducer

Figure 53: Important dimensions of the second prototype (dimensions in mm)

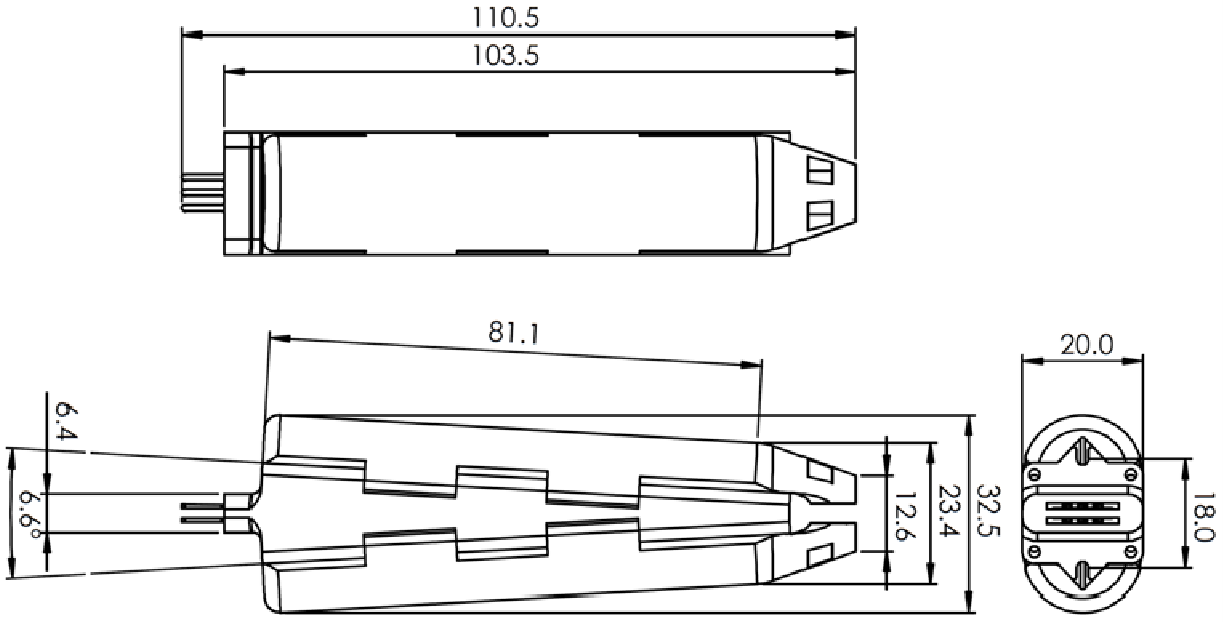

Fatigue Test P-Values

The accuracy/repeatability test and movement resistance test were performed before and after the fatigue cycling of the fatigue test and compared to check for significant differences.

The table below shows the result of the two sample t-test. No result showed significant difference since no t-test showed a value below 0.05.

Table 18: Fatigue test t-value for comparison of the results before and after cycling

	Repeatability(n = 50)	Accuracy(n = 50)	Push Force (n = 5)	Pull Force (n = 5)
2A-L	0.062	0.737	0.743	0.165
2A-R	0.695	0.359	0.947	0.567

Appendix F

Third Prototype Information Summary

This section contains additional relevant information about Prototype 3 not disclosed in the thesis body.

Table 19: Third prototype information summary

Categories	Information
Weight	19g
Process	PolyJet
Materials	Hi-Res VeroWhite, Zinc-plated Steel Torx Thrd-forming Screw, 2-28 Thread, 1/2" Length
Other information	Made to mate with Teleflex Arrow 5-Lumen 8.5Fr central line catheter

Figure 54: Important dimensions of Prototype 3